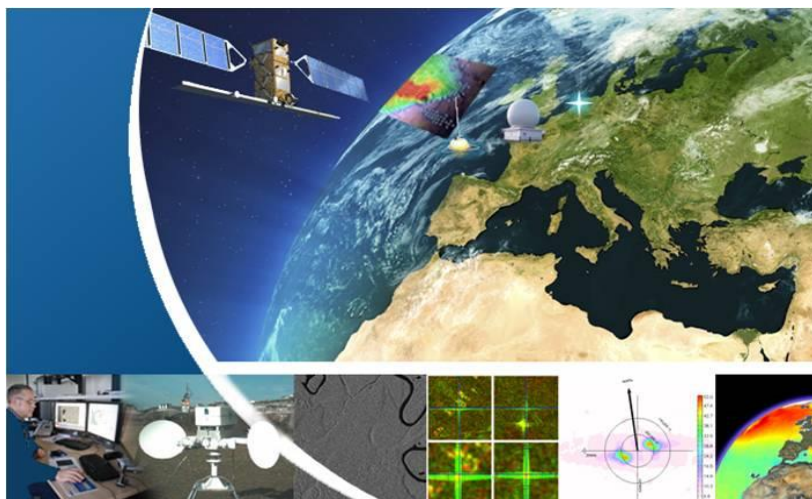




Sentinel-1 Ocean Wind Fields (OWI) Algorithm Definition



Reference: DI-MPC-IPF-OWI

Nomenclature: MPC-0469

2.1 - 13/01/2022



Project funded under the European Union's Copernicus Program.

Copernicus, previously known as GMES (Global Monitoring for Environment and Security), is the European Programme for the establishment of a European capacity for Earth Observation.

The views expressed on this document are those of the authors and do not necessarily represent those of the European Commission.

Open/Public/Público

CHRONOLOGY ISSUES/HISTORIQUE DES VERSIONS

Issue/ Version	Date	Object/Objet	Written by/ Rédigé par	Checked by / Vérfié par
1.0	30/07/10	First issue	A. Mouche	
1.1	08/11/10	<ul style="list-style-type: none"> - Second issue to take into account for ESA RIDs: - RID S1IPFPDR-270, section 1.4 was updated as per RID. - RID S1IPFPDR-262, Motivations on the choice of L1 input files (SLC and/or GRD) are in section 6.2. It is now clear that GRD is the mode for OWI component (except for WV mode) - RID S1IPFPDR-258, As GRD is the default mode for OWI component, issues related to noise correction is now out of the scope. However for L1 SLC (WV mode), noise will be taken into account for wind retrieval. See section 5.1.2. step 3. - RID S1IPFPDR-257, 1- Enhancement of the level of details for the second part of the algorithm. See section 5.2. - 2- Creation of a new section for the overall OCN workflow that is added to the 3 L2 DPMs. See section 3 - 3- Update of table 6-1 (variable naming and origin) - 4- Generic and special function are put in Annex - RID S1IPFPDR-256, harmonization of section 5.2 to be consistent with section 5.1 (inputs, outputs, procedure) - RID S1IPFPDR-255, Section 5.1.2. step 6 has re-written to add details about calibration constant evaluation and monitoring. - RID S1IPFPDR-254, 1- fig. 3.1 has been updated - 2-clarification about the selection of AUX WND/ICE files 	A. Mouche	

		<p>have been added in section 5.1.2 step 4.</p> <ul style="list-style-type: none"> - RID S1IPFPDR-253, - Land mask is derived from AUX_CLM file. It has been changed in the doc accordingly - Section 5.1.2, step 2 has been re-visited to add details and answer questions of this RID. - RID S1IPFPDR-252, This RID related to GRD/SLC issue already addressed. - RID S1IPFPDR-251, Section 5.1.2. step 1 has been revisited to add details and answer questions of this RID. - RID S1IPFPDR-250, general description in section 4 updated. - RID S1IPFPDR-249, functional description in section 5 updated. - RID S1IPFPDR-248, 1/ Case of dual polarization is clarified see section 3 but also section 5.1.2 step 3 - 2/ GRD/SLC issue. See section 6. - 3-4/ OCN section has been added to describe how are organized the outputs of the 3 components a - 5/ Agreed to addition of AUX_CAL to figure 3-1 - 6/ Figure 4-1 updated in updated doc to be clear that creation of the netCDF output file is an additional step not included in the workflow of the OWI component but in the OCN workflow. - RID S1IPFPDR-247, A generic section about OCN has been created - RID S1IPFPDR-246, introduction re-written to clarify purposes of the doc. - RID S1IPFPDR-245, modifications of the doc has been done to get more a readable TOC. - Comments on the dual polarization modes. 		
--	--	---	--	--

MPC-0469

		Details changed according to minor ESA RID		
2.0	06/2019	Introduction of section 5.3 to described OWI inversion unit after IPF 3.10. section 5.2 is renamed to cover Wind inversion unit description for previous IPF version	A. Mouche P. Vincent	G. Hajduch
2.1	13/01/2022	Section 6.2.2 correction on the reference of product specification that is an applicable document - Update of IDL methods used before IPF 2.82 with Python methods. - Addition of CMOD5n implementation in appendix	C. Peureux P. Vincent	

DISTRIBUTION/LISTE DE DIFFUSION

Company/Organisme	Means of distribution/ Format de diffusion	Names/Destinataires



Table of Contents

1	Introduction.....	7
1.1	Purpose.....	7
1.2	Scope.....	7
1.3	Document organisation	7
1.4	Notations and Definitions.....	7
2	Applicable and Reference Documents.....	9
2.1	Applicable Documents.....	9
2.2	Reference Documents.....	10
3	OCN Product Overview	11
3.1	OCN Product Organisation.....	11
3.2	Processing Workflow.....	12
4	OWI Component Overview.....	13
4.1	Calibration & Pre-processing Unit Overview	15
4.2	Inversion Unit Overview	15
5	OWI Functional Description.....	16
5.1	OWI Calibration & Pre-processing Unit	16
5.1.1	Flowchart.....	16
5.1.2	Function and Purpose	17
5.2	OWI – Inversion Unit (before IPF 2.91 included)	32
5.2.1	Flowchart.....	32
5.2.2	Function and Purpose	33
5.3	OWI – Inversion Unit (after IPF 3.10 included)	38
5.3.1	Flowchart.....	38
5.3.2	Function and Purpose	38
6	Input Files.....	41
6.1	Auxiliary Data Files.....	41
6.1.1	Internal Auxiliary Data Files	41
6.1.2	External Auxiliary Data Files.....	41
6.2	SAR Product.....	42
6.2.1	SAR Image.....	42
6.2.2	SAR Product Annotation	44
6.3	Internal Input Parameters	44
6.3.1	Job Order.....	44
6.3.2	Processor Configuration File	44
6.3.3	PRM_LOPin	44
7	List of Symbols.....	45
8	OWI Output Component annotations	48
	Appendix A - Generic and Special Functions	50
	Appendix A 1 - FORMAT_ANGLE	50
	Appendix A 2 - TRIANGULATE – Delaunay Triangulation.....	51
	Appendix A 3 - TRIGRID – Interpolation from Triangulation.....	52
	Appendix A 4 - INTERPOL – Linear 1D Interpolation	54
	Appendix A 5 - BILINEAR – Bilinear Interpolation.....	55
	Appendix A 6 - POLARIZATION_RATIO.....	56
	Appendix A 7 - LOGSIG – Log-Sigmoid Transfer Function.....	58
	Appendix A 8 - CMOD_IFREMER_INVERSE_VECT.....	59

Appendix A 9 - CMOD_IFREMER 63
 Appendix A 10 - CMOD5n..... 66

LIST OF TABLES

Table 5-1 Required Ancillary Wind/Ice Information Used in the Wind Inversion Scheme..... 26
 Table 6-1 Processor Parameters Auxiliary data list for OWI 42
 Table 6-2 L2 Processing Support vs Input L1 Product Characteristics..... 43
 Table 7-1 Variables Used by the Wind Retrieval Algorithm..... 45

LIST OF FIGURES

Figure 3-1 Sentinel-1 L2 Ocean Processing Context Diagram..... 11
 Figure 4-1 High Level OWI Processing Algorithm..... 14
 Figure 5-1 Calibration and Pre-processing Unit Flowchart 17
 Figure 5-2 Data Products Not Converted from Slant Range to Ground Range 19
 Figure 5-3 Kernel Used for the Convolution in the CFAR Algorithm 20
 Figure 5-4 Re-sampling Process of the Ancillary Information onto the SAR Wind Grid 28
 Figure 5-5 Inversion Unit Flowchart (before IPF 2.91) 33
 Figure 5-6 Inversion Unit Flowchart (after IPF 3.10) 38
 Figure 8-1 Log-Sigmoid Transfer Function..... 58
 Figure 8-2 Neural Network Architecture for the Implementation of the Inverse CMOD Scattering Models
 59



1 Introduction

1.1 Purpose

The objective of this document is to define and describe the algorithm implemented in the S1 L2 IPF and the processing steps for the generation of the Ocean Wind Field (OWI) component of the Sentinel-1 Level 2 Ocean (OCN) product.

1.2 Scope

The OCN product contains three sub-products: the OWI component, the Ocean Swell Spectra (OSW) component and the Radial Surface Velocity (RVL) component. This document contains only the OWI algorithm definition. The OSW and RVL algorithm definitions are provided in separate documents (A-10 and A-11).

This document satisfies the PAL2-1 deliverable defined in the Sentinel-1 IPF Statement of Work [A-1] for review at the Sentinel-1 IPF Preliminary Design Review (PDR L2) and Critical Design Review (CDR L1 & L2).

1.3 Document organisation

This document is structured as follows:

Section 1 introduces the purpose, scope, structure and conventions of the document.

Section 2 lists the applicable and reference documents.

Section 3 gives a short L2 OCN product overview.

Section 4 gives the L2 OWI processing system overview.

Section 5 details the functional description of the various OWI processing units.

Section 6 gives a short input data files overview.

Section 7 lists the symbols used to detail the OWI algorithm.

Section 8 gives a short description of the output OWI component structure

Section 9 provides description of generic and special functions used by the OWI algorithm

1.4 Notations and Definitions

The input SAR image is assumed to be in natural SAR coordinates i.e. first line in the file is the first line recorded, and first pixel in the line is the nearest pixel to the satellite. The index x means range direction and y means azimuth direction.

Geographic locations are attached to a given geo-location grid. The following geo-location grid is used in the document:

- $\{lon_i, lat_i\}_{i \in \mathcal{G}_{LADS}}$: The set of longitudes and latitudes such as given in the Geo-location Grid ADS.
- $\{lon_i, lat_i\}_{i \in \mathcal{G}_{SAR\ Wind}}$: The set of longitudes and latitudes for the center of each SAR wind cell

MPC-0469

- $\{lon_i, lat_i\}_{i \in \mathcal{G}_{A \text{ Priori}}}$: The set of longitudes and latitudes defined by the geo-location grid of a priori wind source

The mathematical expressions are all written in SI units.

The following notations are used for truncations:

- *Div*: denotes integer division i.e. the result is truncated to nearest lowest integer.
- *Floor*: denotes truncation to nearest lower integer.
- *Ceil*: denotes truncation to nearest higher integer.
- *Round*: denotes the truncation to nearest integer.

2 Applicable and Reference Documents

2.1 Applicable Documents

- A-1 GMES-DFPR-EOPG-SW-07-00006 Sentinel-1 Product Definitions & Instrument Processing Facility Development Statement of Work, Issue/Revision 4/1, 23-05-2008.
- A-2 Contract Change Notice N. 2, Changes in ESRIN Contract No. 21722/08/I-LG, June 21, 2010
- A-3 BO-024-ESA-0408-RR-1 BOOST Technologies, SAR OCEAN WIND WAVES AND CURRENTS – Review and recommendations for SAR wind, waves and currents retrieval method- Part 1: Wind and Waves (WP 1), Technical report, v 1.0, 08/05/2005
- A-4 BO-024-ESA-0408-RR-2 BOOST Technologies SAR OCEAN WIND WAVES AND CURRENTS – Review and recommendations for SAR wind, waves and currents retrieval method- Part 2: Currents (WP 2), Technical report, BO-024-ESA-0408-RR-2, v 1.0, 08/05/2005
- A-5 BO-024-ESA-0408-ATBD-WP4-wind BOOST Technologies, SAR OCEAN WIND WAVES AND CURRENTS –Algorithm Theoretical Basis Document- Part 1: wind (WP 4), Technical report, v 1.0, 08/05/2005
- A-6 BO-024-ESA-0408-ATBD-WP4-waves BOOST Technologies, SAR OCEAN WIND WAVES AND CURRENTS –Algorithm Theoretical Basis Document – Part 2: waves (WP 4) (WP 4), Technical report, v 1.0, 08/05/2005
- A-7 BO-024-ESA-0408-ATBD-WP5-doppler BOOST Technologies, SAR OCEAN WIND WAVES AND CURRENTS –Algorithm Theoretical Basis Document – Doppler anomaly estimation and analysis (WP 5), Technical report, v 1.3, 08/05/2005
- A-8 BO-024-ESA-0408-VTN BOOST Technologies, SAR OCEAN WIND WAVES AND CURRENTS – Validation Technical Note (WP 6), Technical report, v 1.2, 08/05/2005
- A-9 <http://www.unidata.ucar.edu/software/netcdf/>
- A-10 S1-TN-NRT-52-7450 Sentinel-1 Ocean Swell Wave Spectra (OSW) Algorithm Definition, Issue/Revision 1/1, Nov. 8, 2010, NORUT.
- A-11 S1-TN-NRT- 53-0658 Sentinel-1 L2 Doppler Grid Algorithm Definition, Issue/Revision 1/1, Nov. 8, 2010, NORUT.
- A-12 S1-IC-MDA-52-7454 Sentinel-1 Instrument Processing Facility Interface Control Document, Issue/Revision 1/2, Oct. 27, 2010, MDA.
- A-13 Andersen S., Breivik L.-A., Eastwood S., Godoy O., Lind M., Porires M., Schyberg H., Sea Ice Product Manual, version 3.5, January 2007. <http://www.osi-saf.org/>
- A-14 S1-RS-MDA-52-7441 Sentinel-1 Product Specification, Issue/Revision 2/1, Nov. 5, 2010, MDA.
- A-15 S1-RS-MDA-52-7440 Sentinel-1 Product Definition Document, Issue/Revision: 2/2, Oct. 27, 2010, MDA.
- A-16 S1-RS-MDA-52-7443 Sentinel-1 IPF Auxiliary Product Specification, Issue/Revision 2/1, Nov. 10, 2010, MDA.
- A-17 S1-TN-MDA-52-7445 Sentinel-1 Level 1 Detailed Algorithm Definition, Issue/Revision ½, Aug. 20, 2010, MDA.

2.2 Reference Documents

The following documents provide useful reference information associated with this document. These documents are to be used for information only. Changes to the date/revision number (if provided) do not make this document out of date.

- A-18 Bentamy A., P. Queffeuilou, Y. Quilfen and K. Katsaros, Ocean surface wind fields estimated from satellite active and passive microwave instruments, IEEE Trans. Geosci. Remote Sensing, vol. 37, 2469-2486, 1999
- A-19 Mouche A., D. Hauser, J-F Dalozé, C. Guérin, Dual-Polarization Measurements at C-Band over the Ocean: Results From Airborne Radar Observations and Comparison With ENVISAT ASAR Data, IEEE Trans. Geosci. And Remote Sensing, Volume 43, 753 – 769, 2005
- A-20 Quilfen, Y., B. Chapron, T. Elfouhaily, K. Katsaros and J. Tournadre, Observation of tropical cyclones by high-resolution scatterometry, J. Geophys. Res., Vol. 103, pp. 7767-7786, 1998
- A-21 Thompson, D.R., T.M. Elfouhaily and B. Chapron, Polarization ratio for microwave backscattering from the ocean surface at low to moderate incidence angles, Proc. Int. Geosci. Remote Sens. Symp. 1998
- A-22 Research Systems Inc. (RSI), IDL Reference Guide, Software documentation, 0703IDL60REF, IDL version 6.0, July 2003 Edition, 2003
- A-23 Skolnik, M. I., Radar handbook (McGraw-Hill, 1990), 7.11-7.18
- A-24 P. A. Hwang, B. Zhang, and W. Perrie, Depolarized radar return for breaking wave measurement and hurricane wind retrieval, Geophys. Res. Lett., 37, L01604, doi:10.1029/2009GL041780, 2010
- A-25 Hersbach H., CMOD5n: a C-band geophysical model function for equivalent neutral wind, ECMWF technical memorandum 554, 2008.
- A-26 Komarov A., Komarov S., Buehner M., Ocean Surface Wind Speed Retrieval from the RADARSAT Constellation Mission Co- and Cross-Polarization Images without Wind Direction Input, IEEE Trans. Geosci. Remote Sensing, 2021.

3 OCN Product Overview

The level-2 (L2) ocean product (OCN) has been designed to deliver geophysical parameters related to the wind, waves and surface velocity to a large panel of end-users. The L2 OCN products are estimated from Sentinel-1 (S-1) Synthetic Aperture Radar (SAR) level-1 (L1) products.

L2 OCN products are processed by the level 2 IPF processor and benefit from robust and validated algorithms [A-3,A-4,A-5,A-6,A-7,A-8]. A diagram of the L2 Ocean processing unit context is presented in Figure 3-1.

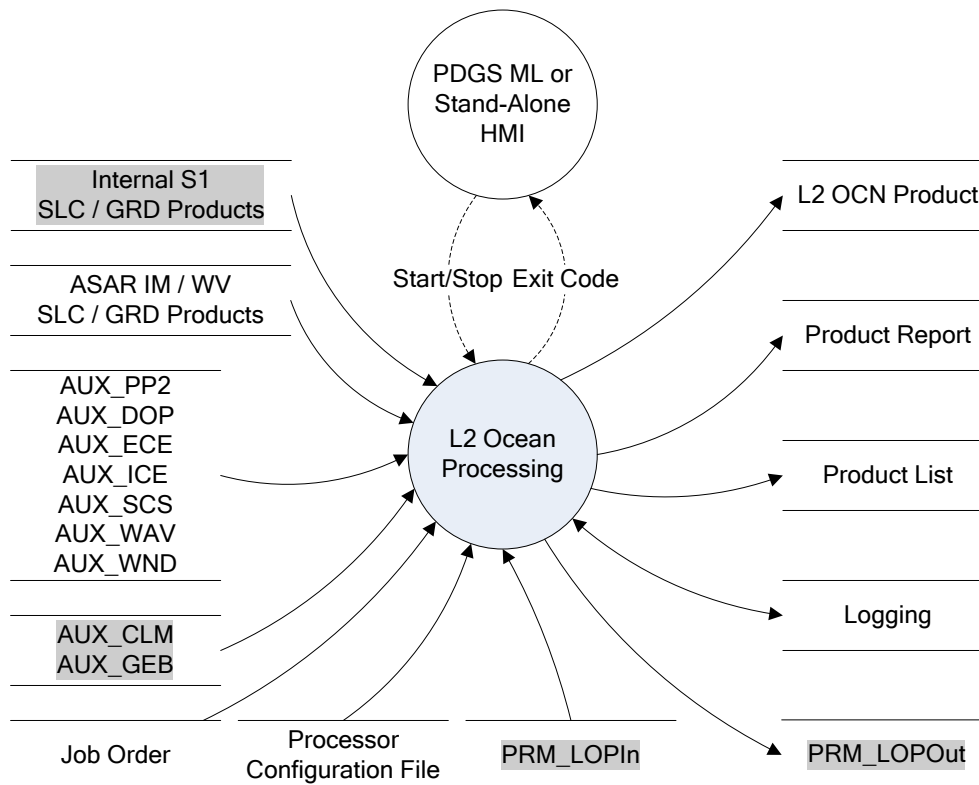


Figure 3-1 Sentinel-1 L2 Ocean Processing Context Diagram

The processor can be used in PDGS environment or in a stand-alone HMI mode. In both cases, a job order is read by the processor to get all high level information required for processing a particular product (e.g. names and directories of input L1 files, names and directories of auxiliary data files, directories of outputs files, etc...). Processing then starts from L1 products using the auxiliary data files provided (e.g. the L2 processor parameter file). During the processing, a log file is generated to monitor the status of each processing step. The final step of the processing is the creation of the product including writing of all the geophysical information into NetCDF files.

3.1 OCN Product Organisation

Each L2 OCN product contains up to three geophysical components: the radial velocity (RVL), the ocean surface wind field (OWI) and the ocean swell spectra (OSW) components. These components are formatted into one output NetCDF file. For SM and WV modes, the L2 product contains all three components. For TOPS mode, the product contains only the RVL and OWI components. The detailed algorithm definition of each component is described in a dedicated document (this document is for OWI and [A-10,A-11] are for OSW and RVL). The output variables corresponding to each component are listed and defined in a dedicated document [A-14].

MPC-0469

For the SM and TOPS modes, the information related to each component is estimated onto a specific grid cell (ground range) whose properties are chosen to optimize the inversion schemes. As a consequence, the SM mode output NetCDF file has three components and the TOPS mode output NetCDF file has two components, each set having its own resolution. In addition, the most pertinent geophysical parameters from RVL and OSW components are interpolated onto the OWI grid to present a set of variables defined at the same resolution. The default value for the resolution of this common grid is 1 km for SM and TOPS modes. The set of variables from RVL and OSW interpolated onto the OWI grid is listed in section 8. RVL and OSW are estimated from an internal L1 SLC product. OWI is estimated from an internal L1 GRD product.

For WV mode, there is no grid. In this case, the resolution of the components is simply the size of the imagette: 20 km. The three components are estimated from internal L1 SLC products.

3.2 Processing Workflow

For SM and TOPS modes, the components are estimated independently. This means that for a given acquired scene, the steps for each component are:

- the appropriate internal L1 product is read,
- the variables corresponding to the considered component are estimated
- a temporary file containing the results is saved locally.

Before IPF 2.82 included, for each component, these three latter steps are executed by different IDL scripts based on the same library of IDL functions. These three scripts are coordinated by a Python script which collects all information mandatory for L2 processing of each component. After IPF 2.84, this processing is performed in Python exclusively with the use of Python SAR data management libraries developed within the MPC, that are still not available to the public.

Then, when it is completed for all components, the components outputs are merged into a single NetCDF file. The same way, for each type of file generated by the three independent scripts, a merging is done.

For WV mode, the three components are estimated sequentially from the same internal L1 SLC product with the same script.

The SM and TOPS modes have the dual-polarization option. However, the L2 OCN components are always estimated only using the information from the co-polarized signal. Thus, the algorithms for each component as well as the workflow for the L2 OCN product generation are not different from that of single polarization product.

4 OWI Component Overview

The Sentinel-1 SAR can be operated in one of the four following nominal acquisition modes:

- Stripmap Mode (SM)
- Interferometric Wide-swath Mode (IW)
- Extra-Wide swath Mode (EW)
- Wave Mode (WV)

The Sentinel-1 wind retrieval processing supports these four nominal acquisition modes.

The Sentinel-1 Level 2 OWI component is an ocean surface wind vector (speed and direction) estimated from a Sentinel-1 Level 1 SAR image by inversion of its associated Normalized Radar Cross Section (NRCS).

In cases of dual-polarization products, cross-polarizations are not used for the wind inversion. Indeed, the state of the art of the Geophysical Model Function (GMF) used to relate sea surface winds to NRCS in VH (or HV) is not mature enough even if a GMF has been recently proposed based on RADARSAT-2 acquisitions [A-26A-24]. Depending on the radiometric quality of the cross-polarizations (SNR) and the progress in the GMF developments, cross-polarization information could be added in the Bayesian scheme to get one single wind field from dual-polarization information. However, the NRCS estimated for each wind cell of the OWI in co- and cross- polarization will be included in the L2 OCN product. In particular, it would enable investigations for the use of the cross-polarization (e.g. better wind characterization).

The OWI component is a set of wind vectors for each processed L1 input product. The norm is wind speed in [m/s] and the argument is wind direction in [degN] (degrees with respect to the North clockwise). The spatial resolution of the vector is directly related to the area on which the NRCS is computed. A part from wind vector, other variables estimated during ocean surface wind inversion such as longitude, latitude, incidence angle, NRCS are included in the L2 product (see section 8. For the full list). Some key sensor parameters of L1 product are also annotated to the product.

The spatial coverage of each wind vector of the OWI component is equal to the spatial coverage of the corresponding L1 WV-SLC or sub-images extracted from the L1 SM or TOPS-GRD product. It is limited to ocean coverage. In the case of the SM or TOPS modes, the L1 product is divided into cells. A wind vector is estimated for each cell leading to a grid for each OWI component variable.

Sentinel-1 wind processing unit system consists of a calibration unit followed by an inversion unit. The calibration unit performs the processing from Level L1 product to a calibrated product containing the parameters required for the wind inversion unit. They are calculated at the resolution of the desired wind cell for each wind cell of the OWI grid. The inversion unit generates the level 2 OWI component using parameters obtained from calibration unit. Figure 4-1 presents a high-level view of the OWI processing algorithm depicting the 2 main steps of the algorithm and the input/output information which are specific to the OWI component of the L2 OCN. Descriptions of the data flow and control/status interfaces can be found in A-12. The list of internal and external auxiliary data used for OWI algorithm is given below in the bullet list. Figure 5-1 and Figure 5-2 give the list of the auxiliary data files used by each unit of the algorithm. Section 5.1.2 and 5.2.2 also detail the needed auxiliary data file at each step of the algorithm.

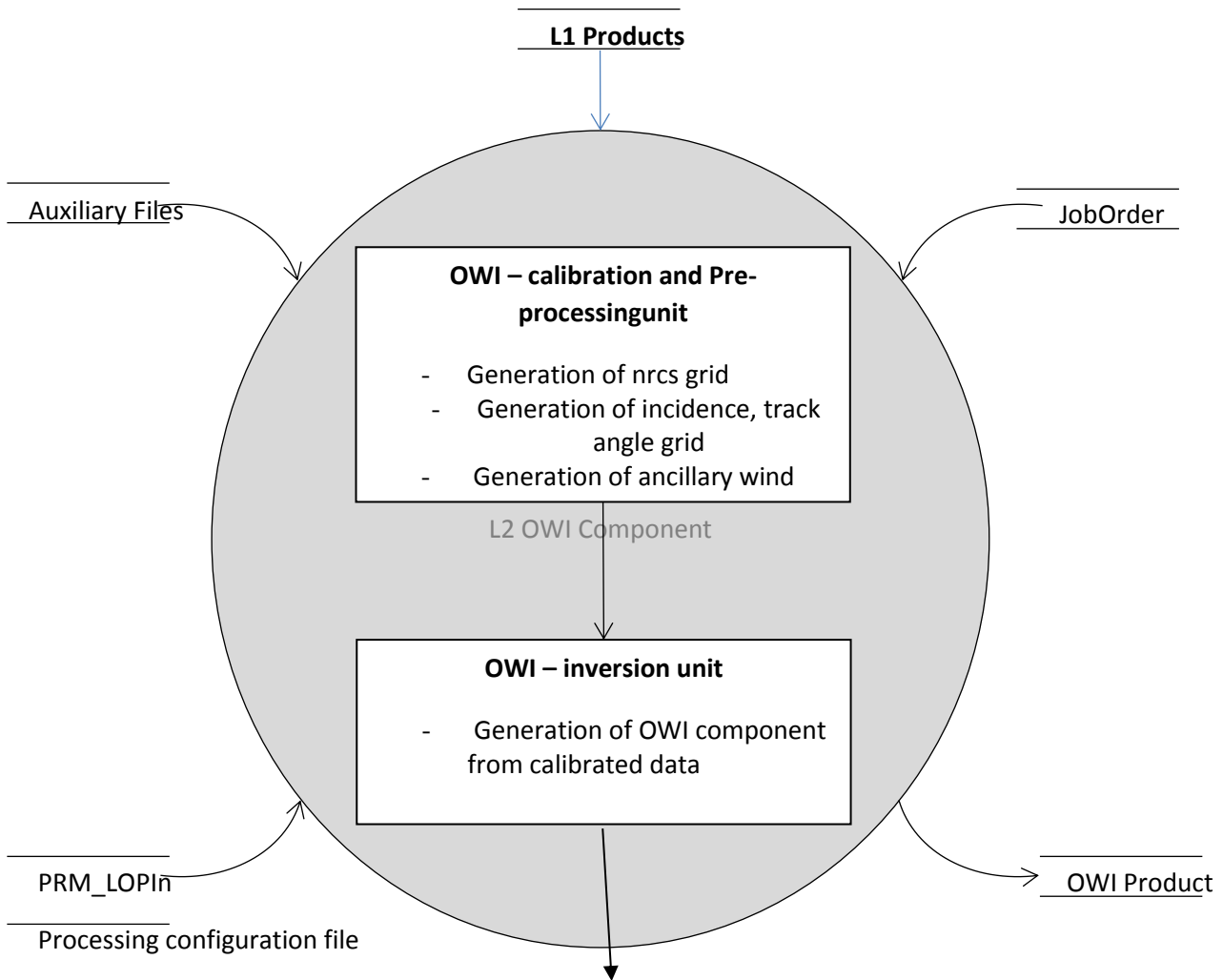


Figure 4-1 High Level OWI Processing Algorithm

The L2 OWI processing system accesses:

- Level 1 internal GRD product
- Auxiliary information (through the auxiliary files) such as
 - coastline data (in case of SM, IW and EW),
 - atmospheric model wind direction,
 - ice mask
 - calibration auxiliary product
 - L2 processor parameters
- Environment parameters like input/output file names and paths to read the appropriate auxiliary files are indicated in the job order.
- The L2 processor set-up parameter file PRM_LOPIn may contain extra processing parameters specific to the OWI algorithm.
- The processor configuration file. It is used to extract the product report/product list extension and the PRM_LOPIn path.

As part of the L2 OCN product, the L2 OWI processing system generates the OWI component which is to be merged with the RVL and OSW (except for TOPS) components in a single NetCDF file after calculations of all components.

4.1 Calibration & Pre-processing Unit Overview

This unit aims at providing all information mandatory for the wind inversion onto the OWI grid.

Before starting the wind retrieval processing, the L2 processor parameters file is read to get the parameters or instructions required to generate the OWI component.

The processing system accesses the external input data, which consists of an S-1 SAR level 1 product.

Given the size in meters of the SAR derived wind cells (indicated in the L2 processor parameters file) and the pixel size in meters (such as read in the data level-1 header), the parameters for the bright target detection, the number of pixels to be averaged in range (x) and azimuth (y) direction are computed. Based on this, the parameters of the OWI are estimated. Arrays corresponding to the intensity image, NRCS, longitude and latitude, incidence angle, track angle, 2-way slant range time and the percentage of pixels in SAR image detected as bright targets are generated.

The a priori wind and ice mask information from ancillary data are interpolated on the SAR OWI grid.

In addition, an internal calibration constant based on ancillary geophysical parameters is calculated for each SAR Image product.

4.2 Inversion Unit Overview

The purpose of this unit is to estimate the wind vector using NRCS values, the incidence angles, the track angles and the a priori wind and ice information. This inversion is performed using statistical Bayesian inference.

The inversion scheme is slightly different between VV and HH polarization. HH polarization requires one additional step where the NRCS in HH is transformed to a VV equivalent NRCS. In the case of dual polarization data, the cross-polarization NRCS is not used in the wind inversion scheme.

Eventually, the SAR-derived wind field is merged with the RVL and OSW components into a single NetCDF file to get the OCN product in S-1 format as described in A-14.

The main information delivered by the OWI component is a wind vector (direction, norm) for each wind cell of the OWI grid. However, the product also contains the incidence angle, the latitude/longitude, track angle, corresponding to the center of the grid cell and the NRCS. In addition, some of the information of the RVL and OSW (except for TOPS) components is re-sampled on the OWI grid. The merging steps and the re-sampling steps constitute the final step of the L2 OCN processing.

5 OWI Functional Description

This section describes the processing steps performed to derive the OWI component of the OCN product

5.1 OWI Calibration & Pre-processing Unit

The calibration and pre-processing unit extract a sub-image (except for WV where one single wind vector is estimated for the product) from the L1 SLC image product, performs the bright target detection and estimates the NRCS, incidence and track angles. The estimation is repeated over the number sub-images related to the resolution of the wind field expected.

5.1.1 Flowchart

Figure 5-1 shows the flowchart of the calibration and pre-processing unit. The three types of input data are described in section 6.

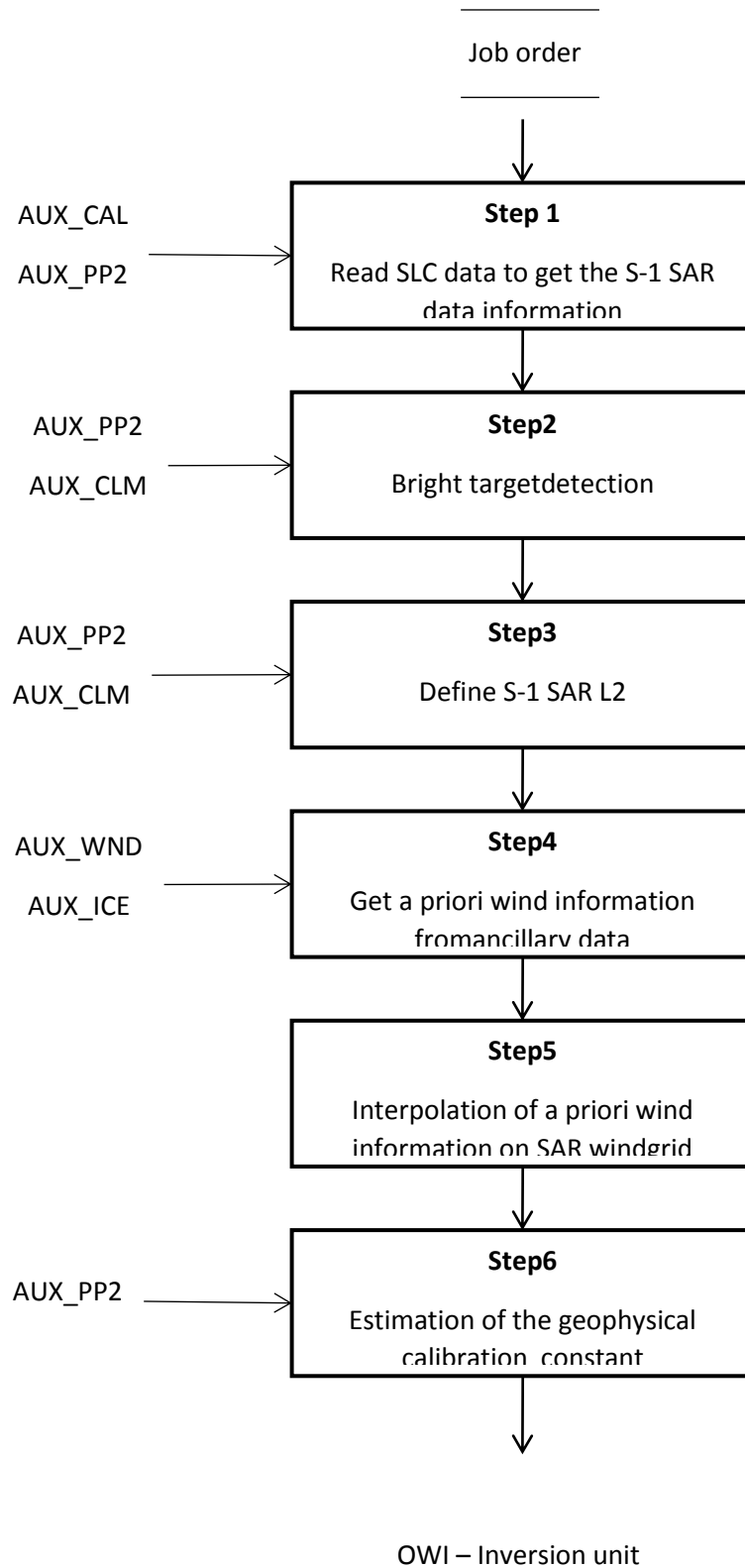


Figure 5-1 Calibration and Pre-processing Unit Flowchart

5.1.2 Function and Purpose

The different processing steps in the flowchart are described below.



Step 1: Get SAR data information

The aim of this step is to read the L1 product to get SAR data information and parameters pertinent for wind inversion

Input parameters:

fname: The absolute path and filename of the path-oriented S-1 SAR level-1 data product to be processed. This is a string parameter read from the Job order.

Output parameters:

L_x^I, L_y^I :	Number of range and azimuth pixels in the level-1 image.
P_x^I, P_y^I :	Image pixel size in meters in range and azimuth direction.
$\{(x, y)_i\}_{i \in \mathcal{G}_{LADS}}$	Arrays (M,N) of index tie points given by the geo-Location grid.
$\{lon_i, lat_i\}_{i \in \mathcal{G}_{LADS}}$:	Arrays (M,N) of longitude and latitudes at tie points $\{(x, y)_i\}_{i \in \mathcal{G}_{LADS}}$.
$\{t_i\}_{i \in \mathcal{G}_{LADS}}$:	Array (M,N) of two-way slant range times at tie points $\{(x, y)_i\}_{i \in \mathcal{G}_{LADS}}$, only until IPF 2.82 included.
$\{\theta_i\}_{i \in \mathcal{G}_{LADS}}$:	Array (M,N) of incidence angles at tie points $\{(x, y)_i\}_{i \in \mathcal{G}_{LADS}}$
K^c :	The calibration vectors (accordingly to the updates along the azimuth direction), LUT
P_{TXRX}^{ol} :	The Transmitter/Receiver polarization.
Φ :	The satellite ground track direction (direction between the platform heading and the North).
F^{srg} :	Flag set to 1 if slant-range-to-ground-range conversion is applied.
T_0 :	UTC time of first pixel of first line (early azimuth).
R^A :	The aspect ratio
P_x^G, P_y^G :	Ground pixel size corrected for aspect ratio

M and N denote respectively the dimensions of the index ties point matrices according to range and azimuth directions.

Procedure:

1. The array $\{\theta_i\}_{i \in \mathcal{G}_{LADS}}$ is re-sampled onto SAR pixels grid of the whole SAR image (for all modes SM, IW, EW or WV) $\mathcal{G}_{SAR \text{ Image}}$ to compute θ_c the incidence angle at index location (x_c, y_c) ¹ corresponding to the center of the image:

$$\begin{cases} x_c = (L_x^I - 1)/2 \\ y_c = (L_y^I - 1)/2 \end{cases} \quad (1)$$

2. The image ground pixel size in range direction is computed as follows:

¹ Indexes (x_c, y_c) can have fractional values if L_x (resp. L_y) are even.

$$P_x^G = \begin{cases} P_x^I & \text{if } F^{srgr} = 1 \\ \frac{P_x^I}{\sin \theta_c} & \text{if } F^{srgr} = 0 \end{cases} \quad (2)$$

3. The aspect ratio value is given by:

$$R^A = \frac{P_x^G}{P_y^I} \quad (3)$$

4. The image ground pixel size in azimuth direction (after correction for aspect ratio) is computed as follows:

$$P_y^G = R^A \cdot P_y^I \quad (4)$$

Figure 5-2 shows the case of data products not converted from slant range to ground range. The use of the aspect ratio parameter R^A aims at preserving a “realistic” looking aspect in compressing R^A pixels in the azimuth directions. As a result the compressed ground pixel is nearly square.

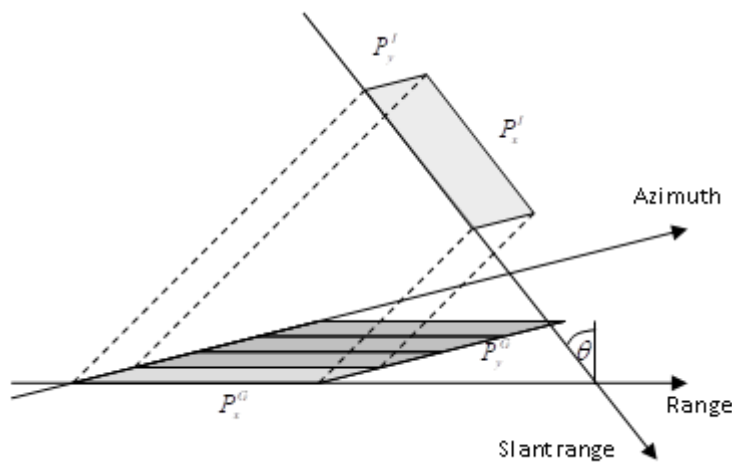


Figure 5-2 Data Products Not Converted from Slant Range to Ground Range

Step 2: Bright target detection

The aim of this step is to produce a mask of detected targets which must not be taken into account in the NRCS calculation for wind inversion. This mask has the same resolution as the SAR image (L_x, L_y).

Metal structures like ships and oil rigs can cause strong echoes in SAR images, which are not wind signatures and lead to overestimation of the wind speed. Thus, it is necessary to detect these bright targets in the image and remove them before calculating the NRCS over each wind cell. For each SAR image pixel where a bright target has been detected, the mask of detected targets is set to 1 and equals 0 otherwise.

This detection is based on the Constant False Alarm Rate (CFAR) algorithm, which is an adaptive filter A-23. It consists in comparing, for each pixel of the SAR image, its amplitude with respect to the one of the pixels in its vicinity. The choice of an adaptive filter is motivated by the fact that an absolute threshold cannot be chosen since the sea surface clutter measured by the SAR is changing depending on several parameters such as the wind field and incidence angle which vary within the SAR image.

The main assumptions justifying the use of this algorithm are:

1. The targets to detect are brighter than the surrounding ocean clutter.
2. The statistical properties of sea surface can be estimated on the image to be processed.

- Image subsets values are a mixture of two different statistical phenomena: homogeneous sea surface clutter alone on one side and homogeneous sea surface clutter with bright targets on the other side.

The filter consists in a convolution of the SAR image pixels located over the sea using a kernel separated in three regions, centered on the potential target, as shown in Figure 5-3:

- The target window, containing the image pixel under investigation,
- The background area, containing image pixels of the sea surface and possibly some bright targets,
- The buffer area, which purpose is to leave enough space between the background area and the target window so that any large target within the target window is not taken into account in the background statistics.

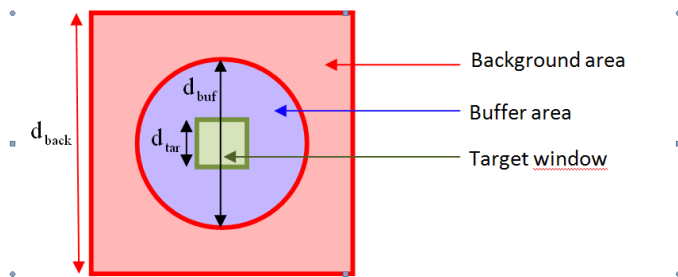


Figure 5-3 Kernel Used for the Convolution in the CFAR Algorithm

Input parameters:

- P_x^G, P_y^G : Image ground pixel size corrected for aspect ratio computed at Step 1.
- $\{(DN^I)_i\}_{i \in \mathcal{G}_{SAR Image}}$: Digital number at each SAR image pixel $\{(x, y)_i\}_{i \in \mathcal{G}_{SAR Image}}$
- $\{(M^I)_i\}_{i \in \mathcal{G}_{SAR Image}}$: Mask array containing land flag at each SAR Image pixel $\{(x, y)_i\}_{i \in \mathcal{G}_{SAR Image}}$
- p_{fa} : The probability of false alarm read in the AUX_PP2 file. It depends on several parameters and will be calibrated using a set of test SAR images. Prior to this, default value is 10^{-7} .

Output parameters:

- $\{(B^I)_i\}_{i \in \mathcal{G}_{SAR Image}}$: Mask array of bright targets at each SAR Image pixel $\{(x, y)_i\}_{i \in \mathcal{G}_{SAR Image}}$. Set to 1 if detected and 0 if not.
- $\{(A^I)_i\}_{i \in \mathcal{G}_{SAR Image}}$: The amplitude values at each SAR image pixel $\{(x, y)_i\}_{i \in \mathcal{G}_{SAR Image}}$

Procedure:

- The digital numbers are converted into amplitude for SLC product

$$\{(A^I)_i\}_{i \in \mathcal{G}_{SAR Image}} = \begin{cases} \{|DN^I|_i\}_{i \in \mathcal{G}_{SAR Image}}, & \text{for SLC products} \\ \{(DN^I)_i\}_{i \in \mathcal{G}_{SAR Image}}, & \text{for GRD products} \end{cases}$$

- The mask of land is interpolated onto SAR grid using the same method than used in step 5 to interpolated wind/ice information.



3. The sizes of the different windows in the convolution kernel, d_{back} , d_{buf} and d_{tar} , are defined according to the image ground pixel size P_x^G, P_y^G , with $d_{\text{back}} > d_{\text{buf}} > d_{\text{tar}}$:
- d_{tar} equals one pixel
 - d_{buf} depends on the pixel spacing of the SAR image mode of acquisition. It is adjusted so that the largest targets in the target window will not be part of the background window. d_{buf} is chosen so that it could cover the largest super tankers, which can reach up to 350 meters.
 - d_{back} should be sufficiently large to allow good statistics over the background area and should not ever be too large not to include any other bright targets inside the background window. Empirical optimization used in ENVISAT should be used.

$$d_{\text{bac}_x} = \sqrt{2} \left(2 + \frac{3}{2} \frac{350}{\min(\text{res}_x)} \right) + 1,$$

$$d_{\text{bac}_y} = \sqrt{2} \left(2 + \frac{3}{2} \frac{350}{\min(\text{res}_y)} \right) + 1,$$

, where $\min(\text{res}_x)$ and $\min(\text{res}_y)$ are respectively the minimum resolution of the SAR product along the range and azimuth axis in meters.

4. Edges of the SAR image amplitude are extended with median values in order to avoid side effects during the convolution.
5. Let $\{(H^k)_i\}_{i \in G_{\text{Kernel}}}$ be the kernel with elements equal to 1 inside the background area and 0 elsewhere and n^k the number of strictly positive elements in the kernel. Then, for each pixel of the SAR image considered $\{(M_b^I)_i\}_{i \in G_{\text{SAR image}}}$, the mean and $\{(S_b^I)_i\}_{i \in G_{\text{SAR image}}}$, the standard deviation of the background area are computed. These operations can be summarized by a single convolution of the SAR image amplitude by the kernel:

$$M_b^I = \frac{A^I \otimes H^K}{n^K} \quad (5)$$

$$S_b^I = \sqrt{\frac{(A^I)^2 \otimes H^K}{n^K} - (M_b^I)^2} \quad (6)$$

6. Considering that the background distribution is modeled by a Gaussian with a mean of 0 and a standard deviation of 1, the cut-off value c is computed for each the SAR image pixel location (x,y) so that the probability that a random variable is lesser than c equals p_{fa} . In other words, c is the solution of the following equation:

$$p_{fa} = \int_c^{+\infty} \frac{1}{\sqrt{2\pi}} e^{-\frac{x^2}{2}} dx \quad (7)$$

Let P_f be the function defined by:

$$P_f(u) = \int_u^{+\infty} \frac{1}{\sqrt{2\pi}} e^{-\frac{x^2}{2}} dx = \frac{1}{2} - \int_0^u \frac{1}{\sqrt{2\pi}} e^{-\frac{x^2}{2}} dx$$

As P_f is a strictly decreasing function, it is bijective. The unique antecedent of p_{fa} , c , can be found using discrete values of u :

$$c = \underset{u \in \mathbb{N}}{\operatorname{argmin}} [|p_{fa} - P_f(u)|]$$

7. Then, the mask array $\{(B^I)_i\}_{i \in \mathcal{G}_{\text{SAR Image}}}$ is defined at each SAR Image pixel location (x,y) as follows:

$$B^I(x, y) = \begin{cases} 1, & \text{if } \frac{A^I(x,y) - M_b^I(x,y)}{S_b^I(x,y)} > c \\ 0 & \text{otherwise} \end{cases} \quad (8)$$

Step 3: Define wind inversion inputs

This step aims at defining the set of variables directly used for the wind inversion. Except for the WV mode, most of these variables are a set of variables calculated at the resolution of OWI grid. This resolution is given by the wind cell size (typically 1x1 km for the image modes).

Input parameters:

- P^W : The approximate size of SAR derived wind cells in meter. This parameter is returned by the field cell_size in AUX_PP2. The final size in range and azimuth direction of the SAR derived wind cells may not match exactly P^W . Indeed, the number of SAR image pixels to be averaged in range and azimuth direction must be integer values.
- P_x^G, P_y^G : Image ground pixel size corrected for aspect ratio computed at Step 1.
- R^A : The aspect ratio computed at Step 1
- $\{(x, y)_i\}_{i \in \mathcal{G}_{\text{LADS}}}$: Arrays (M,N) of index tie points given by the geo-Location grid such as read at Step 1.
- $\{lon_i, lat_i\}_{i \in \mathcal{G}_{\text{LADS}}}$: Arrays (M,N) of longitude and latitudes at tie points $\{(x, y)_i\}_{i \in \mathcal{G}_{\text{LADS}}}$ such as read at Step 1.
- $\{t_i\}_{i \in \mathcal{G}_{\text{LADS}}}$: Array (M,N) of two-way slant range times at tie points $\{(x, y)_i\}_{i \in \mathcal{G}_{\text{LADS}}}$ such as read at Step 1.
- $\{\theta_i\}_{i \in \mathcal{G}_{\text{LADS}}}$: Array (M,N) of incidence angles at tie points $\{(x, y)_i\}_{i \in \mathcal{G}_{\text{LADS}}}$ such as read at Step 1.
- K^c : The calibration constant such as read at Step 1.
- $\{(A^I)_i\}_{i \in \mathcal{G}_{\text{SAR Image}}}$: The amplitude values at each SAR image pixel $\{(x, y)_i\}_{i \in \mathcal{G}_{\text{SAR Image}}}$, computed at step 2
- $\{(B^I)_i\}_{i \in \mathcal{G}_{\text{SAR Image}}}$: Mask array at each SAR Image pixel $\{(x, y)_i\}_{i \in \mathcal{G}_{\text{SAR Image}}}$ of bright targets computed at step 2.

M and N denote respectively the dimensions of the index ties point matrices according to range and azimuth directions.

Output parameters:

- S^f : The sampling factor which determines how many pixels will be averaged in range (and azimuth) direction to approximately match the expected wind cell size P^W .
- P_x^W, P_y^W : Wind cell size in meters in range and azimuth directions
- L_x^W, L_y^W : Number of range and azimuth wind cells in the SAR derived wind field

Each one of the following parameters is calculated at the centre of each SAR derived wind cells of the OWI grid. They are matrices.

- $\{(x, y)_i\}_{i \in \mathcal{G}_{\text{SAR Wind}}}$: The index values
- $\{lon_i, lat_i\}_{i \in \mathcal{G}_{\text{SAR Wind}}}$: Longitude and latitude
- $\{(A^W)_i\}_{i \in \mathcal{G}_{\text{SAR Wind}}}$: Averaged amplitude values
- $\{t_i\}_{i \in \mathcal{G}_{\text{SAR Wind}}}$: Two-way slant range times
- $\{\theta_i\}_{i \in \mathcal{G}_{\text{SAR Wind}}}$: Incidence angles

The following parameters are calculated for each cell of the OWI grid considering all the pertinent information of the considered cell. They are matrices.

- $\{(\sigma^0)_i\}_{i \in \mathcal{G}_{\text{SAR Wind}}}$: NRCS
- $\{(M^W)_i\}_{i \in \mathcal{G}_{\text{SAR Wind}}}$: Mask array containing flag at each SAR wind cell (i.e. at points $\{(x, y)_i\}_{i \in \mathcal{G}_{\text{SAR Wind}}}$). Flag values are set to 1 for all non valid wind vector estimates (presence of land, null values, etc).
- $\{(B^W)_i\}_{i \in \mathcal{G}_{\text{SAR Wind}}}$: Array of the percentage of bright targets detected in the SAR image pixels used for the computation of SAR wind pixel $\{(x, y)_i\}_{i \in \mathcal{G}_{\text{SAR Wind}}}$

Procedure:

1. The sampling factor is defined as follows:

$$S^f = \text{round} \left(\frac{P^W}{\min([P_x^G, P_y^G])} \right) \quad (9)$$

2. The wind cell size in meters in range and azimuth directions can now be computed:

$$\begin{cases} P_x^W &= S^f \cdot P_x^G \\ P_y^W &= S^f \cdot P_y^G \end{cases} \quad (10)$$

3. The number of wind cells in range and azimuth direction is given by:

$$\begin{cases} L_x^W &= \frac{L_x^I}{S^f} = \frac{L_x^I}{S_x^f} \\ L_y^W &= \frac{L_y^I}{(S^f \cdot R^A)} = \frac{L_y^I}{S_y^f} \end{cases} \quad (11)$$

Where $S_x^f = S^f$ and $S_y^f = S^f \cdot R^A$

4. The index values corresponding to the centre of SAR wind cells are given by:

$$\begin{cases} \{x_i\}_{i \in \mathcal{G}_{\text{SAR Wind}}} &= \left\{ \frac{(S_x^f - 1)}{2} + i \cdot S_x^f \right\}_{0 \leq i \leq (L_x^W - 1)} \\ \{y_i\}_{i \in \mathcal{G}_{\text{SAR Wind}}} &= \left\{ \frac{(S_y^f - 1)}{2} + i \cdot S_y^f \right\}_{0 \leq i \leq (L_y^W - 1)} \end{cases} \quad (12)$$

5. Longitudes and latitudes $\{lon_i, lat_i\}_{i \in \mathcal{G}_{\text{SAR Wind}}}$ at each SAR wind cells can now be computed from $\{(x, y)_i\}_{i \in \mathcal{G}_{\text{LADS}}}$ and $\{lon_i, lat_i\}_{i \in \mathcal{G}_{\text{LADS}}}$ using any 2D interpolation method.

IDL procedure for IPF until IPF2.82 included

In the delivered IDL-based SAR wind retrieval prototype (which uses Delaunay A-22), the following IDL command are applied, IDL is used until IPF 2.82 included :

$$\text{triangulate}(x, y, \text{triangles}) \quad (13)$$

$$\begin{cases} \text{lon} = \text{trigrd}(x, y, \text{longrid}, \text{triangles}, \text{GS}, \text{limits}, / \text{QUINTIC}) \\ \text{lat} = \text{trigrd}(x, y, \text{latgrid}, \text{triangles}, \text{GS}, \text{limits}, / \text{QUINTIC}) \end{cases} \quad (14)$$

Where:

$$\begin{aligned} x &= \{x_i\}_{i \in \mathcal{G}_{LADS}} \\ y &= \{y_i\}_{i \in \mathcal{G}_{LADS}} \\ \text{longrid} &= \{\text{lon}_i\}_{i \in \mathcal{G}_{LADS}} \\ \text{latgrid} &= \{\text{lat}_i\}_{i \in \mathcal{G}_{LADS}} \\ \text{GS} &= [S^f, S^f \cdot R^A] = [S_x^f, S_y^f] \\ \text{limits} &= \left[\left(\frac{S_x^f - 1}{2} \right), \left(\frac{S_y^f - 1}{2} \right), \left(\frac{S_x^f - 1}{2} \right) + (L_x^W - 1) \cdot S_x^f, \left(\frac{S_y^f - 1}{2} \right) + (L_y^W - 1) \right. \\ &\quad \left. \cdot S_y^f \right] \\ \text{lon} &= \{\text{lon}_i\}_{i \in \mathcal{G}_{\text{SAR Wind}}} \\ \text{lat} &= \{\text{lat}_i\}_{i \in \mathcal{G}_{\text{SAR Wind}}} \end{aligned}$$

Python procedure since IPF2.84 and later

Longitudes and latitudes are computed from an extension of the rational polynomial coefficients method using the ground control points embedded in the L1 product and Python Gdal CoordinateTransformation method from the pixel/line image coordinates $x = \{x_i\}_{i \in \mathcal{G}_{\text{SAR Wind}}}$ and $y = \{y_i\}_{i \in \mathcal{G}_{\text{SAR Wind}}}$ EPSG 4326 coordinates, resulting in $\text{lon} = \{\text{lon}_i\}_{i \in \mathcal{G}_{\text{SAR Wind}}}$ and $\text{lat} = \{\text{lat}_i\}_{i \in \mathcal{G}_{\text{SAR Wind}}}$.

6. For each wind cell of the OWI grid, the averaged amplitude value $A^W(x, y)$ at the SAR wind cell location (x, y) is computed from the SAR image pixels amplitude values A^I where no bright target were detected as follows:

$$A^W(x, y) = \sqrt{\frac{1}{n} \sum_{k=x \cdot S_x^f}^{(x+1) \cdot S_x^f - 1} \left(\sum_{l=y \cdot S_y^f}^{(y+1) \cdot S_y^f - 1} (A^I(k, l) B^I(k, l))^2 \right)}$$

$$\text{where } n = \sum_{k=x \cdot S_x^f}^{(x+1) \cdot S_x^f - 1} \left(\sum_{l=y \cdot S_y^f}^{(y+1) \cdot S_y^f - 1} B^I(k, l) \right)$$

7. For each wind cell of the OWI grid, the percentage of pixels in SAR image detected as bright targets among those used in the computation of SAR wind cell at location $\{(x, y)_i\}_{i \in \mathcal{G}_{\text{SAR Wind}}}$ is computed as follows:

$$B^W(x, y) = \frac{100}{S_x^f S_y^f} \sum_{k=x \cdot S_x^f}^{(x+1) \cdot S_x^f - 1} \left(\sum_{l=y \cdot S_y^f}^{(y+1) \cdot S_y^f - 1} (B^I(k, l)) \right) \quad (15)$$

8. Two-way slant range times computation

IDL procedure for IPF until IPF2.82 included

For the OWI grid, two-way slant range times $\{t_i\}_{i \in \mathcal{G}_{\text{SAR Wind}}}$ at each SAR wind cells can now be computed from $\{(x, y)_i\}_{i \in \mathcal{G}_{\text{LADS}}}$ and $\{t_i\}_{i \in \mathcal{G}_{\text{LADS}}}$ as follows:

$$t = \text{trigrd}(x, y, tgrid, triangles, GS, limits, /QUINTIC) \quad (16)$$

Where:

$$\begin{aligned} tgrid &= \{t_i\}_{i \in \mathcal{G}_{\text{LADS}}} \\ t &= \{t_i\}_{i \in \mathcal{G}_{\text{SAR Wind}}} \end{aligned}$$

Python procedure since IPF2.84 and later

Two-way slant range times are not computed anymore.

9. IDL procedure for IPF until IPF2.82 included

For the OWI grid, incidence angles $\{\theta_i\}_{i \in \mathcal{G}_{\text{SAR Wind}}}$ at each SAR wind cells can now be computed from $\{(x, y)_i\}_{i \in \mathcal{G}_{\text{LADS}}}$ and $\{\theta_i\}_{i \in \mathcal{G}_{\text{SAR LADS}}}$ as follows:

$$theta = \text{trigrd}(x, y, thetagrid, triangles, GS, limits, /QUINTIC) \quad (17)$$

Where:

$$\begin{aligned} thetagrid &= \{\theta_i\}_{i \in \mathcal{G}_{\text{LADS}}} \\ theta &= \{\theta_i\}_{i \in \mathcal{G}_{\text{SAR Wind}}} \end{aligned}$$

Python procedure since IPF2.84 and later

Incidence angles $theta = \{\theta_i\}_{i \in \mathcal{G}_{\text{SAR Wind}}}$ are computed from the bilinear spline interpolation of L1 annotation files at the corresponding $\{(x, y)_i\}_{i \in \mathcal{G}_{\text{SAR Wind}}}$ locations.

10. For the OWI grid, NRCS values $\{(\sigma^0)_i\}_{i \in \mathcal{G}_{\text{SAR Wind}}}$ at each SAR wind cells can now be computed from $\{(A^W)_i\}_{i \in \mathcal{G}_{\text{SAR Wind}}}$ and the calibration LUT contained in the L1 product using formulation given in A-17.

For both GRD and SLC products,

$$\{(\sigma^0)_i\}_{i \in \mathcal{G}_{\text{SAR Wind}}} = \frac{\{(A^W)_i^2\}_{i \in \mathcal{G}_{\text{SAR Wind}}}}{\{(lutsigma0)_i\}_{i \in \mathcal{G}_{\text{SAR Wind}}}}$$

Where $\{(lutsigma0)_i\}_{i \in \mathcal{G}_{\text{SAR Wind}}}$ is the NRCS calibration LUT .

For S-1, the thermal noise is given in the thermal noise power LUT and has to be applied before the calibration step. This thermal noise is azimuth, range and swath dependent.

For SLC product, by definition, the thermal noise cannot be already removed. In cases of L1 SLC products accepted as input of the L2 OWI algorithm (i.e. WV mode), the noise effect is corrected before applying calibration procedure using the thermal noise power correction given in the L1 product.

In case of GRD products, the thermal noise should have already been removed. If the thermal noise correction has not been performed, then it is taken into account using the thermal noise power correction given in the L1 product.

In case of dual-polarization products, the NRCS is calculated for both channels even if only the co-polarization is used for inversion.

11. For the OWI grid, a mask $\{(M^W)_i\}_{i \in \mathcal{G}_{\text{SAR Wind}}}$ is derived for each SAR wind cells using longitudes and latitudes $\{\text{lon}_i, \text{lat}_i\}_{i \in \mathcal{G}_{\text{SAR Wind}}}$ (land flagging) and $\{(\sigma^0)_i\}_{i \in \mathcal{G}_{\text{SAR Wind}}}$ (null values).

$$M^W(x, y) = \begin{cases} 1 & \text{if } (\{\text{lon}(x, y), \text{lat}(x, y)\} \text{ is on land}) \text{ OR } (\sigma^0(x, y) \text{ EQ } 0) \\ 0 & \text{else} \end{cases} \quad (18)$$

Step 4: Get a priori wind/ice information

This step aims at reading wind and ice ancillary data which are co-located (or the closest) in time with the SAR acquisition. Auxiliary data file for wind and ice information are only selected according to the acquisition time. Once it is done the information inside the selected auxiliary files are chosen to be in agreement with the geographical area covered by the SAR product. It means there is no need to have geographical information about the product when selecting AUX_WND/AUX_ICE files.

Wind and ice ancillary information are not given on the same geo-location grid than the SAR image and not necessarily given on the same geo-location grid source. The grid of ancillary data is noted $\mathcal{G}_{\text{A Priori}}$ for both ice and wind even it can be different.

It does not matter whether geo-location grid of ancillary wind/ice source $\mathcal{G}_{\text{A Priori}}$ are similar or regular. This wind/ice information will be further interpolated onto SAR wind grid $\mathcal{G}_{\text{SAR wind}}$ (Step 5).

Table 5-1 summarizes the information necessary to perform the wind field inversion.

Table 5-1 Required Ancillary Wind/Ice Information Used in the Wind Inversion Scheme

Field	Description	Unit
Ancillary Wind		
<i>vector</i>	An IDL structure containing fields <i>u</i> and <i>v</i>	-
<i>vector.u</i>	Vector (or equivalently 1D array) containing zonal wind component (i.e. the wind component along the local parallel or latitude towards East direction) of ancillary wind vector	m/s
<i>vector.v</i>	Vector (or equivalently 1D array) containing meridional wind component (i.e. the wind component along the local meridian or longitude towards North direction) of ancillary wind vector	m/s
<i>anclon</i>	Vector (or equivalently 1D array) containing corresponding longitude values	degree
<i>anclat</i>	(or equivalently 1D array) containing corresponding latitude values	degree
<i>xstime</i>	Time of the predicted wind field.	UTC
Ancillary Ice		
<i>ice mask</i>	Vector (or equivalently 1D array) containing corresponding indicator of ice, sea or land for the corresponding location	-
<i>quality flag</i>	Vector (or equivalently 1D array) containing corresponding indicator of the quality of the ice mask	-
<i>anclon</i>	Vector (or equivalently 1D array) containing corresponding longitude values	degree
<i>anclat</i>	(or equivalently 1D array) containing corresponding latitude values	degree
<i>xstime</i>	Time of the given ice information.	UTC

The zonal component of the wind vector is the component along the parallels (from west to east). The meridional component of the wind vector is the component along the meridians (from South to North). The reason of returning zonal and meridional ancillary wind components instead of wind speed and direction is driven by the interpolation onto SAR wind grid that will be performed at next step (the interpolation of wind directions, which are 360°-cyclic, is not a trivial problem).

Input parameters:

$\{lon_i, lat_i\}_{i \in \mathcal{G}_{SAR\ Wind}}$: The set of longitudes and latitudes at each SAR wind cells (i.e. at points $\{(x, y)_{i \in \mathcal{G}_{SAR\ Wind}}\}$) such as computed in Step 3.

T_0 : UTC time of first pixel of first line (early azimuth) such as read in Step 1.

Output parameters:

$\{(lon_{AP})_i, (lat_{AP})_i\}_{i \in \mathcal{G}_{A\ Priori}}$: Longitude and latitude values of points where ancillary wind/ice information is available.

$\{(u_{AP})_i, (v_{AP})_i, (l_{AP})_i\}_{i \in \mathcal{G}_{A\ Priori}}$: zonal and meridional components of ancillary wind and ice information

Procedure:

The selection and reading procedure of ancillary wind/ice information is dependent upon the choice (or the availability) of ancillary wind/ice information.

- The selection of the AUX files depends only upon the temporal sampling of ancillary wind/ice fields as well as the naming convention of wind/ice data files. For wind, the spatial and temporal coverage are expected to be respectively not more than 0.5° x 0.5° and 6 hours. For ice the spatial coverage are expected to be respectively not more than 10 km x 10 km and 1 day.
- The reading procedure depends on data format (NetCDF, GRIB, HDF, PDS format, etc). Several formats can coexist for ancillary data such as the ice product. However, the software only support the one corresponding to the auxiliary data files defined in [A-12]

Only the following requirement must be satisfied:

1. Ancillary wind/ice data must be selected such that it is the closest in time to the SAR data acquisition, here defined by the parameter T_0 .
2. Location points where ancillary wind/ice information is available must surround the geographical limits of the coverage area of the SAR level-1 data. This will avoid errors resulting from extrapolation.

Step 5: Interpolation of a priori wind/ice information

This step aims at interpolating the a priori wind/ice information onto the OWI grid. The interpolation of the ancillary a priori wind/ice information is performed in two steps such as shown in Figure 5-4:

Step 5.1: Delaunay triangulation to transform irregularly sampled NWP wind model/ice information outputs onto regular lon/lat grid.

Step 5.2: Bilinear interpolation of the regularly transformed NWP a priori information/ ice information onto the SAR wind grid².

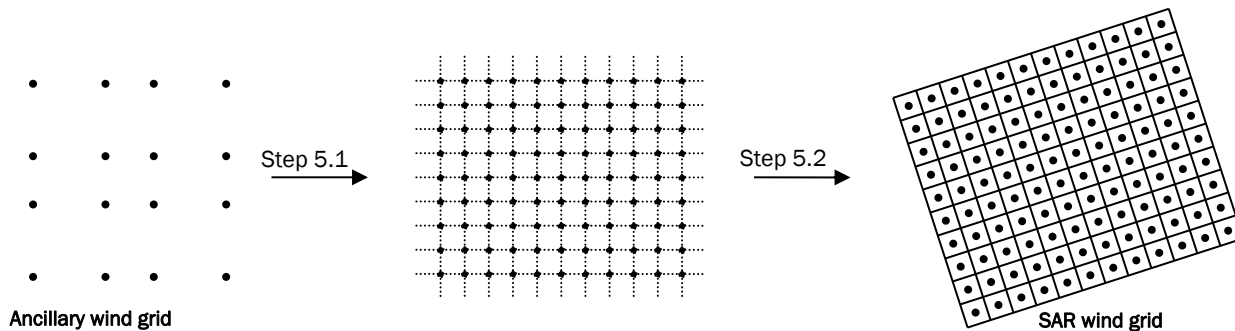


Figure 5-4 Re-sampling Process of the Ancillary Information onto the SAR Wind Grid

Input parameters:

- $\{lon_i, lat_i\}_{i \in \mathcal{G}_{SAR\ Wind}}$: The set of longitudes and latitudes at each SAR wind cells (i.e. at points $\{(x, y)_i\}_{i \in \mathcal{G}_{SAR\ Wind}}$) such as computed in Step 3.
- $\{(lon_{AP})_i, (lat_{AP})_i\}_{i \in \mathcal{G}_{A\ Priori}}$: Longitude and latitude values of points where ancillary wind/ice information is available such as read in Step 4.
- $\{(u_{AP})_i, (v_{AP})_i, (l_{AP})_i\}_{i \in \mathcal{G}_{A\ Priori}}$: zonal and meridional components of ancillary wind information as well as ice mask information such as read in Step 4

Output parameters:

- $\{(u_{AP})_i, (v_{AP})_i, (l_{AP})_i\}_{i \in \mathcal{G}_{SAR\ Wind}}$: zonal and meridional components of ancillary wind information as well as ice mask re-sampled on SAR Wind grid $\mathcal{G}_{SAR\ wind}$.
- $\{(U_{AP})_i\}_{i \in \mathcal{G}_{SAR\ Wind}}$: The ancillary wind speed re-sampled on SAR wind grid $\mathcal{G}_{SAR\ wind}$.
- $\{(\phi_{AP})_i\}_{i \in \mathcal{G}_{SAR\ Wind}}$: The ancillary wind direction re-sampled on SAR wind grid $\mathcal{G}_{SAR\ wind}$.

Procedure:

IDL procedure for IPF until IPF2.82 included:

1. $\{(u_{AP})_i, (v_{AP})_i, (l_{AP})_i\}_{i \in \mathcal{G}_{A\ Priori}}$ will first be interpolated onto a regular lon/lat grid using IDL triangulation/interpolation (Step 5.1):

$triangulate, x, y, triangles, boundaryPts$ (19)

² Two-dimensional interpolation based on krigging approach using IDL KRIG2D function A-22 has also been tested. However, it was found that this method is much more time consuming with no evident benefit.



$$\begin{cases} ugrid = \text{trigrd}(x, y, u_{AP}, \text{triangles}, GS, \text{limits}, \text{EXTRAPOLATE}=\text{boundaryPts}, XGRID = lon_g, YGRID = lat_g) \\ vgrid = \text{trigrd}(x, y, v_{AP}, \text{triangles}, GS, \text{limits}, \text{EXTRAPOLATE}=\text{boundaryPts}, XGRID = lon_g, YGRID = lat_g) \\ lgrid = \text{trigrd}(x, y, l_{AP}, \text{triangles}, GS, \text{limits}, \text{EXTRAPOLATE}=\text{boundaryPts}, XGRID = lon_g, YGRID = lat_g) \end{cases} \quad (20)$$

where:

$$\begin{aligned} x &= \{(lon_{AP})_i\}_{i \in \mathcal{G}_{A \text{ Priori}}} \\ y &= \{(lat_{AP})_i\}_{i \in \mathcal{G}_{A \text{ Priori}}} \\ u_{AP} &= \{(u_{AP})_i\}_{i \in \mathcal{G}_{A \text{ Priori}}} \\ v_{AP} &= \{(v_{AP})_i\}_{i \in \mathcal{G}_{A \text{ Priori}}} \\ l_{AP} &= \{(l_{AP})_i\}_{i \in \mathcal{G}_{A \text{ Priori}}} \\ \Delta_{lon} &= \text{abs}(\{lon(1,0)\}_{\mathcal{G}_{SAR \text{ Wind}}} - \{lon(0,0)\}_{\mathcal{G}_{SAR \text{ Wind}}}) \\ \Delta_{lat} &= \text{abs}(\{lat(0,1)\}_{\mathcal{G}_{SAR \text{ Wind}}} - \{lat(0,0)\}_{\mathcal{G}_{SAR \text{ Wind}}}) \\ GS &= [\Delta_{lon}, \Delta_{lat}] \\ \text{limits} &= [\min(\{lon_i\}_{i \in \mathcal{G}_{SAR \text{ Wind}}}), \min(\{lat_i\}_{i \in \mathcal{G}_{SAR \text{ Wind}}}), \max(\{lon_i\}_{i \in \mathcal{G}_{SAR \text{ Wind}}}), \max(\{lat_i\}_{i \in \mathcal{G}_{SAR \text{ Wind}}})] \end{aligned}$$

lon and lat denotes the x and y grids as returned by the trigrd IDL function and corresponding to $ugrid$ and $vgrid$ variables.

- $ugrid$ and $vgrid$ will then be interpolated onto SAR wind grid $\mathcal{G}_{SAR \text{ wind}}$. (Step 5.2) to provide $\{(u_{AP})_i, (v_{AP})_i, (l_{AP})_i\}_{i \in \mathcal{G}_{SAR \text{ Wind}}}$ as follows:

$$\begin{cases} x_{lon} = \text{interpol}(x, lon_g, lon) \\ y_{lat} = \text{interpol}(y, lat_g, lat) \end{cases} \quad (21)$$

Where:

$$\begin{aligned} x &= [0 \dots (\text{size}(lon_g) - 1)]_{\mathbb{N}} \\ lon &= \{lon_i\}_{i \in \mathcal{G}_{SAR \text{ Wind}}} \\ y_{lat} &= [0 \dots (\text{size}(lat_g) - 1)]_{\mathbb{N}} \\ lat &= \{lat_i\}_{i \in \mathcal{G}_{SAR \text{ Wind}}} \end{aligned}$$

And:

$$\begin{cases} u = \text{BILINEAR}(ugrid, x_{lon}, y_{lat}) \\ v = \text{BILINEAR}(vgrid, x_{lon}, y_{lat}) \\ l = \text{BILINEAR}(lgrid, x_{lon}, y_{lat}) \end{cases} \quad (22)$$

Where:

$$\begin{aligned} u &= \{(u_{AP})_i\}_{i \in \mathcal{G}_{SAR \text{ Wind}}} \\ v &= \{(v_{AP})_i\}_{i \in \mathcal{G}_{SAR \text{ Wind}}} \\ l &= \{(l_{AP})_i\}_{i \in \mathcal{G}_{SAR \text{ Wind}}} \end{aligned}$$

- The ancillary wind speed re-sampled on SAR wind grid $\{(U_{AP})_i\}_{i \in \mathcal{G}_{SAR \text{ Wind}}}$ is given by:

$$\{(U_{AP})_i\}_{i \in \mathcal{G}_{SAR \text{ Wind}}} = \sqrt{(\{(u_{AP})_i\}_{i \in \mathcal{G}_{SAR \text{ Wind}}})^2 + (\{(v_{AP})_i\}_{i \in \mathcal{G}_{SAR \text{ Wind}}})^2} \quad (23)$$

- The ancillary wind direction re-sampled on SAR wind grid $\{(\phi_{AP})_i\}_{i \in \mathcal{G}_{SAR \text{ Wind}}}$ is obtained by:

$$\{(\phi_{AP})_i\}_{i \in \mathcal{G}_{SAR \text{ Wind}}} = 90 - \arctan\left(\frac{\{(v_{AP})_i\}_{i \in \mathcal{G}_{SAR \text{ Wind}}}}{\{(u_{AP})_i\}_{i \in \mathcal{G}_{SAR \text{ Wind}}}}\right) \quad (24)$$

Previous steps 1 and 2 have been simplified using GDAL interpolation method.

Ancillary is directly read as a Gdal dataset. The interpolation of the ancillary data on the gridded SAR product grid is done as:

$$gdal.ReprojectImage(ds, dst_ds, src_srs_wkt, dst_srs_wkt, interp_type)$$

where

ds : GDAL object to take relative to ancillary data relative to either $\{(u_{AP})_i, (v_{AP})_i, (l_{AP})_i\}_{i \in \mathcal{G}_{A \text{ Priori}}}$

dst_ds : GDAL object relative to the SAR re-gridded product

src_srs_wkt : WTK of the SRS of the ancillary data

dst_srs_wkt : WKT of the SRS relative to the re-gridded SAR product

$Interp_type$: default=`gdal.GRA_Cubic` for ECMWF wind ancillary and `gdal.GRA_NearestNeighbour` for OSISAF

Step 3 and 4 remain common.

Step 6: Calibration factor monitoring

This step aims at estimating the calibration constant based on the geophysical ancillary data. There are two objectives :

- First, to get a quality flag for the calibration constant of the image considered. As the calibration constant estimate is based on the analysis of one single product, it is a very rough indicator of the calibration constant. Only images with a severe issue concerning the calibration procedure should be detected by this flag.
- Second, to monitor the calibration constant of S-1 during on a long term basis. In particular, evolution of the calibration constant with respect to time could be monitored for each mode using the L2 OCN products acquired during long period.

The calibration quality flag is based on comparisons between NRCS as estimated from S-1 level 1 products and NRCS as predicted using a geophysical model function combined with wind ancillary data. There is one value per level 2 OWI component.

The calibration constant used for the long term monitoring is a vector with respect to incidence angle. For each wind cell, a calibration constant is estimated. Then for each line of the image in the radial direction, a single calibration constant is estimated along the azimuth direction.

Input parameters:

 $\{(\sigma^0)_i\}_{i \in \mathcal{G}_{SAR \text{ Wind}}}$:

The NRCS at each SAR wind cell as calculated in step 3

 $\{\theta_i\}_{i \in \mathcal{G}_{SAR \text{ Wind}}}$:

The incidence angle at each SAR wind cell as calculated in step 3

$\{(M^W)_i\}_{i \in \mathcal{G}_{SAR\ Wind}}$:	Mask array containing flag at each SAR wind cell (i.e. at points $\{(x, y)_i\}_{i \in \mathcal{G}_{SAR\ Wind}}$). Flag values are set to 1 for all non valid wind vector estimates (presence of land, null values, etc). This mask is estimated in step 4.
$\{(U_{AP})_i, (\varphi_{AP})_i, (\tau_{AP})_i\}_{i \in \mathcal{G}_{SAR\ Wind}}$:	The ancillary wind speed/direction w.r.t. radar looking direction and ice information re-sampled on SAR wind grid $\mathcal{G}_{SAR\ wind}$ in step 5
<i>Threshold_Qflag_Kc</i> :	Value above which the estimated NRCS from the S-1 data information and parameters is considered as non-acceptable read in AUX_PP2 file. The default value is 1.35 dB (3 times the RMS of the calibration factor as found using ASAR WSM images) but could be updated in the future.
<i>Gmf_index</i>	: index from AUX_PP2 file to choose the GMF. The choice of the GMF is triggered by the AUX_PP2. By default, the GMF used is CMOD-IFR2 and later CMOD5n (from IPF 3.10)

Output parameters:

$\{(\overline{\sigma^0})_i\}_{i \in \mathcal{G}_{SAR\ Wind}}$:	The NRCS estimated at each SAR wind cell for the given ancillary wind information.
K_{GeoCal}^I :	Geophysical calibration constant directly estimated from the wind auxiliary data (1 value).
$K_{GeoCal}^{monitoring}(x)$:	Geophysical calibration constant directly estimated from the wind auxiliary data for long term monitoring (1 vector of Nx values).
$Q_{K_{GeoCal}^C}^{flag}$:	Calibration quality flag

Procedure:

1. The ancillary wind speed and direction re-sampled on SAR wind grid are used to predict the expected NRCS for each wind cell of the OWI grid given the satellite track angle, incidence angle and polarization using CMOD empirical scattering model (also called GMF) and polarization ratio (PR) (for HH polarization) :

$$\begin{aligned} \bar{\sigma}_{VV}^0 \Big|_{i \in \mathcal{G}_{SAR\ Wind}} &= GMF(\theta_i, (U_{AP})_i, (\varphi_{AP})_i, gmf_index) \Big|_{i \in \mathcal{G}_{SAR\ Wind}}, \text{ if VV} \\ \bar{\sigma}_{HH}^0 \Big|_{i \in \mathcal{G}_{SAR\ Wind}} &= \frac{GMF(\theta_i, (U_{AP})_i, (\varphi_{AP})_i, gmf_index)}{PR(\theta_i, (U_{AP})_i, (\varphi_{AP})_i)} \Big|_{i \in \mathcal{G}_{SAR\ Wind}}, \text{ if HH} \end{aligned}$$

2. From the predicted and estimated NRCS the geophysical calibration constant are derived. The equation depends on the calibration procedure. Let $\{K_{GeoCal}(x, y)\}_{i \in \mathcal{G}_{SAR\ Wind}}$ be the calibration constant derived for all cell grids at location x, y inside the grid.

The geophysical calibration constant unique value for the product considered is given by:

$$K_{GeoCal}^I = \frac{\sum_{x=0, y=0}^{N_x, N_y} K_{GeoCal}(x, y) |M^{SAR\ wind}(x, y) - 1| |\tau^{SAR\ wind}(x, y) - 1|}{\sum_{x=0, y=0}^{N_x, N_y} |M^{SAR\ wind}(x, y) - 1| |\tau^{SAR\ wind}(x, y) - 1|},$$

where N_x and N_y are respectively the number of rows and columns.

The geophysical calibration constant vector for the product considered is given by:

$$K_{\text{GeoCal}}^{\text{monitoring}}(x) = \frac{\sum_{y=0}^{N_y} K_{\text{GeoCal}}(x, y) |M^{\text{SAR wind}}(x, y) - 1| |\tau^{\text{SAR wind}}(x, y) - 1|}{\sum_{y=0}^{N_y} |M^{\text{SAR wind}}(x, y) - 1| |\tau^{\text{SAR wind}}(x, y) - 1|}$$

3. The geophysical calibration constant is used to qualify the calibration constant.

If $K_{\text{GeoCal}}^I > \text{Threshold_Qflag_Kc}$,

$$\text{then } Q_{K_{\text{Geophysical}}^C}^{\text{flag}} = 0 \text{ else } Q_{K_{\text{Geophysical}}^C}^{\text{flag}} = 1$$

5.2 OWI – Inversion Unit (before IPF 2.91 included)

The inversion unit derives the wind speed and direction from the NRCS, incidence and track angles obtained from L1 product and *a priori* information from ancillary data.

5.2.1 Flowchart

Figure 5-5 shows the flowchart of the inversion unit (before IPF 2.91).

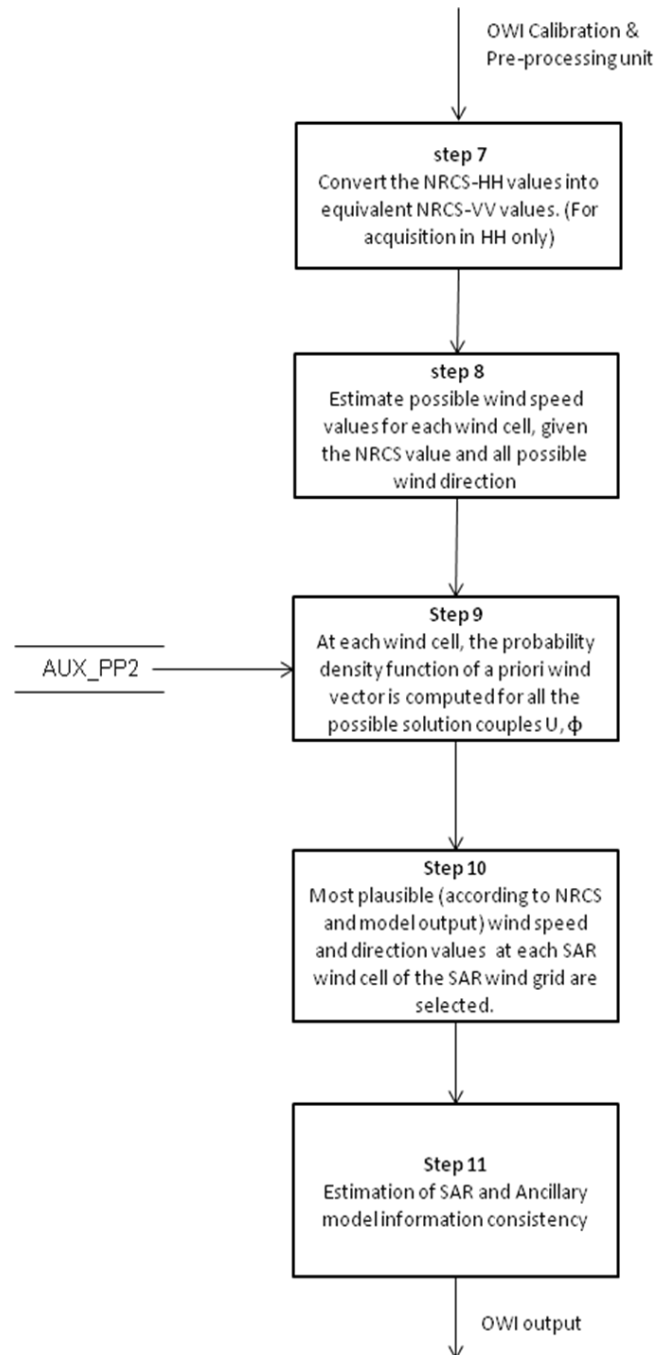


Figure 5-5 Inversion Unit Flowchart (before IPF 2.91)

5.2.2 Function and Purpose

At this level, the parameters of the wind vector are estimated using statistical Bayesian inversion. The different processing steps in the flowchart are described below.

Step 7: Convert the NRCS-HH (for acquisition in HH only)

This step aims at converting the NRCS acquired in HH polarization into equivalent NRCS acquired in VV polarization for each grid cell of the OWI grid.

Input parameters:

- $\{\theta_i\}_{i \in \mathcal{G}_{\text{SAR Wind}}}$: The incidence angle at each SAR wind cell from step 3
- $\{(\varphi_{AP})_i\}_{i \in \mathcal{G}_{\text{SAR Wind}}}$: The ancillary wind speed and (corrected) wind direction w.r.t. radar looking direction re-sampled on SAR wind grid $\mathcal{G}_{\text{SAR wind}}$ from step 5

Output parameters:

- $\{(\sigma_{VV}^0)_i\}_{i \in \mathcal{G}_{\text{SAR Wind}}}$: The VV- equivalent NRCS estimated at each SAR wind cell

Procedure:

Since the empirical scattering model that is used for the wind retrieval inversion has been derived only for VV-polarized data, the NRCS of SAR images that have been acquired in HH-pol configuration must be transformed into equivalent VV-pol NRCS values:

$$(\sigma_{VV}^0)_i = \begin{cases} (\sigma^0)_i & , \text{ if VV} \\ (\sigma^0)_i \cdot \text{PR}(\theta_i, (\varphi_{AP})_i) & , \text{ if HH} \end{cases} \quad (25)$$

Details about the polarization ratio can be found in section Appendix A 6 -.

Step 8: Estimate Space of Solutions

For each grid cell of the OWI grid, this step aims at estimating the space of solutions for the wind speed and wind direction given the equivalent NRCS-VV, incident angle and antenna look-angle.

Input parameters:

- $\{\theta_i\}_{i \in \mathcal{G}_{\text{SAR Wind}}}$: The incidence angle at each SAR wind cell from step 3
- $\{(\varphi_{AP})_i\}_{i \in \mathcal{G}_{\text{SAR Wind}}}$: The ancillary wind speed and (corrected) wind direction w.r.t. radar looking direction re-sampled on SAR wind grid $\mathcal{G}_{\text{SAR wind}}$ from step 5
- $\{(\sigma_{VV}^0)_i\}_{i \in \mathcal{G}_{\text{SAR Wind}}}$: The VV- equivalent NRCS estimated at each SAR wind cell from step 7

Output parameters:

- $\{(\{U\}, \{\varphi\})_i\}_{i \in \mathcal{G}_{\text{SAR Wind}}}$: The space of solution for the wind speeds and directions each SAR wind cell

Procedure:

For each wind cell of the OWI grid, given the normalized radar cross section $(\sigma_{VV}^0)_i$, the incidence angle θ_i and all possible wind direction (with respect to antenna look angle) φ , the ensemble of possible wind speed solution is simulated using neural network implementation of the inverse GMF (see section Appendix A 8 -):

$$\{U\}_{i \in \mathcal{G}_{\text{SAR Wind}}} = \text{GMF}^{-1}(\theta, \sigma_{VV}^0, \{(\varphi)_{i \in \mathcal{G}_{\text{SAR Wind}}}\}) \quad (26)$$

Step 9: Probability density function of the ancillary wind

This step aims at estimating the probability density function of the ancillary wind information for each wind cell of the OWI grid.

Input parameters:

- $\{(U_{AP})_i, (\phi_{AP})_i\}_{i \in \mathcal{G}_{\text{SAR Wind}}}$: The ancillary wind speed and wind direction w.r.t. radar looking direction re-sampled on SAR wind grid $\mathcal{G}_{\text{SAR wind}}$ from step 5
- $\sigma_{U_{AP}}$: The uncertainty associated to the wind speed of the ancillary wind expressed in [m/s] read in AUX_PP2 file.
- $\sigma_{\phi_{AP}}$: The uncertainty associated to the wind direction of the ancillary wind expressed in degrees read in AUX_PP2 file.
- $\{(\{U\}, \{\phi\})\}_{i \in \mathcal{G}_{\text{SAR Wind}}}$: The space of solution for the wind speeds and directions found at each SAR wind cell in step 8.

Output parameters:

- $f_{\mathbf{u}_{AP}}(\mathbf{u})$: Probability density function of a priori wind vectors at each grid cell of the OWI grid given the space of solution for the wind speeds and directions estimated at each SAR wind cell from the measured NRCS.
- $\{(\{U\}, \{\phi\})\}_{i \in \mathcal{G}_{\text{SAR Wind}}}$: The space of solution for the wind speeds and directions found at each SAR wind cell in step 8.

Procedure:

At each wind cell of the OWI grid, the probability density function of a priori wind vector is computed for all the possible solution couples $\{(U, \phi)_i\}_{i \in \mathcal{G}_{\text{SAR Wind}}}$:

$$f_{\mathbf{u}_{AP}}(\mathbf{u}) = f_{U_{AP}}(U) \cdot f_{\phi_{AP}}(\phi) \quad (27)$$

Where :

$$f_{U_{AP}}(U) = \frac{1}{\sqrt{2\pi\sigma_{U_{AP}}^2}} \exp\left[-\frac{(U-(U_{AP})_i)^2}{2\sigma_{U_{AP}}^2}\right]$$

$$f_{\phi_{AP}}(\phi) = \frac{1}{\sqrt{2\pi\sigma_{\phi_{AP}}^2}} \exp\left[-\frac{\text{format_angle}(\phi-(\phi_{AP})_i)^2}{2\sigma_{\phi_{AP}}^2}\right]$$

and the values of $\sigma_{U_{AP}}$ and $\sigma_{\phi_{AP}}$ given in the AUX_PP2 file.

To get these analytical formulae for the probability density function of the ancillary wind component, we assume that the wind speed and direction are independent variables and that the probability to get a correct a priori wind information is given by Gaussian law with a standard deviation (respectively by $\sigma_{U_{AP}}$ and $\sigma_{\phi_{AP}}$ for the wind speed and direction).

Step 10: Wind vector estimation

This step aims at estimating the most plausible (according to the NRCS and model output) wind speed and direction values at each SAR wind cell of OWI grid.

Input parameters:

$f_{u_{AP}}(\mathbf{u})$: Probability density function of a priori wind vectors at each grid cell of the OWI grid given the space of solution for the wind speeds and directions estimated at each SAR wind cell from the measured NRCS. It is estimated at step 9.

$\{(\{U\}, \{\varphi\})\}_{i \in \mathcal{G}_{SAR\ Wind}}$: The space of solution for the wind speeds and directions found at each SAR wind cell in step 8.

Output parameters:

$\{U_i, \varphi_i\}_{i \in \mathcal{G}_{SAR\ Wind}}$: The estimated wind speed and wind direction values at each SAR wind cell of the SAR wind grid.

Procedure:

The estimated wind speed and wind direction (w.r.t. the line-of-sight direction of the antenna) values $\{(\{U\}, \{\varphi\})\}_{i \in \mathcal{G}_{SAR\ Wind}}$ at each SAR wind cell of the SAR wind grid are selected such that they satisfy the following equation:

$$(U, \varphi)_{i \in \mathcal{G}_{SAR\ wind}} = \underset{-(180/\Delta\varphi) \leq \varphi < (180/\Delta\varphi)}{\operatorname{argmin}} \{|\ln| [f_{U_{AP}}(U) \cdot f_{\varphi_{AP}}(\varphi)]|\} \quad (28)$$

The estimated wind direction (according to meteorological convention, i.e. the direction from which the wind is blowing) is given by:

$$\phi_i = \operatorname{format_angle}(90 + \phi - \varphi_i) \quad (29)$$

The format_angle function is described in section Appendix A -.

Step 11: Inversion quality flag

This step aims at evaluating the consistency between the NRCS as measured by the SAR and the a priori wind information for each wind cell for the OWI grid. Information on the consistency between NRCS and a priori wind is also combined to the percentage of bright target inside each wind cell and to the calibration quality indicator to get a indicator of the quality of the inversion for each wind cell of the OWI grid.

Input parameters:

$f_{u_{AP}}(\mathbf{u})$: Probability density function of a priori wind vectors at each grid cell of the OWI grid given the space of solution for the wind speeds and directions estimated at each SAR wind cell from the measured NRCS. It is estimated at step 9.

$\{(\{U\}, \{\varphi\})\}_{i \in \mathcal{G}_{SAR\ Wind}}$: The space of solution for the wind speeds and directions found at each SAR wind cell in step 8.

$\{(B^W)_i\}_{i \in \mathcal{G}_{\text{SAR Wind}}}$: Percentage of bright targets detected in the SAR image at each grid cell as calculated in step 2
$Threshold_Qflag_inversion$: Value above which minimization in the inversion is considered as low quality from AUX-PAR file
$Threshold_Qflag_Kc$: Value above which the calibration of the product is considered as badly calibrated from AUX-PAR file
$Threshold_Pb$: Value above which the NRCS estimated at the SAR wind cell resolution is considered as low quality from AUX-PAR file

Output parameters:

$\{(Q_{inversion})_i\}_{i \in \mathcal{G}_{\text{SAR Wind}}}$: Consistency between ancillary model output and NRCS used in the wind inversion scheme.
$\{(Q_{wind}^{flag})_i\}_{i \in \mathcal{G}_{\text{SAR Wind}}}$: Quality flag at each SAR wind cell

Procedure:

The value of the estimated minimum of

$$\{(Q_{inversion})_i\}_{i \in \mathcal{G}_{\text{SAR Wind}}} = \min_{-\left(\frac{180}{\Delta\varphi}\right) \leq j < \left(\frac{180}{\Delta\varphi}\right)} \{|\ln[f_{U_{AP}}(U) \cdot f_{\varphi_{AP}}(\varphi)]|\} \quad (30)$$

gives an indication about the consistency between the various information used in the inversion scheme. The lower is the minimum the better is the consistency and the higher must be the confident level of the inverted wind vector.

Then $\{(Q_{inversion})_i\}_{i \in \mathcal{G}_{\text{SAR Wind}}}$, and $\{(B^W)_i\}_{i \in \mathcal{G}_{\text{SAR Wind}}}$ are combined to produce a wind quality flag at each wind cell.

$$\begin{aligned} \{(Q_{wind}^{flag})_i\}_{i \in \mathcal{G}_{\text{SAR Wind}}} &= 1, \text{ if } \{(Q_{inversion})_i\}_{i \in \mathcal{G}_{\text{SAR Wind}}} > Threshold_Qflag_inversion \\ &= 2, \text{ if } \{(B^W)_i\}_{i \in \mathcal{G}_{\text{SAR Wind}}} > Threshold_Pb \\ &= 3, \text{ if } K_{GeoCal}^I > Threshold_Qflag_inversion \\ &= 4, \text{ if } \{(Q_{inversion})_i\}_{i \in \mathcal{G}_{\text{SAR Wind}}} > Threshold_Qflag_inversion \text{ and} \\ &\quad \{(B^W)_i\}_{i \in \mathcal{G}_{\text{SAR Wind}}} > Threshold_Pb \\ &= 5, \text{ if } K_{GeoCal}^I > Threshold_Qflag_Kc \text{ and} \\ &\quad \{(Q_{inversion})_i\}_{i \in \mathcal{G}_{\text{SAR Wind}}} > Threshold_Qflag_inversion \\ &= 6, \text{ if } K_{GeoCal}^I > Threshold_Qflag_Kc \text{ and} \\ &\quad \{(B^W)_i\}_{i \in \mathcal{G}_{\text{SAR Wind}}} > Threshold_Pb \\ &= 7, \text{ if } K_{GeoCal}^I > Threshold_Qflag_Kc \text{ and} \\ &\quad \{(Q_{inversion})_i\}_{i \in \mathcal{G}_{\text{SAR Wind}}} > Threshold_Qflag_inversion \text{ and} \\ &\quad \{(B^W)_i\}_{i \in \mathcal{G}_{\text{SAR Wind}}} > Threshold_Pb \end{aligned}$$

5.3 OWI – Inversion Unit (after IPF 3.10 included)

The inversion unit derives the wind speed and direction from the NRCS, incidence and track angles obtained from L1 product and *a priori* information from ancillary data.

5.3.1 Flowchart

Figure 5-6 shows the flowchart of the inversion unit (after IPF 3.10).

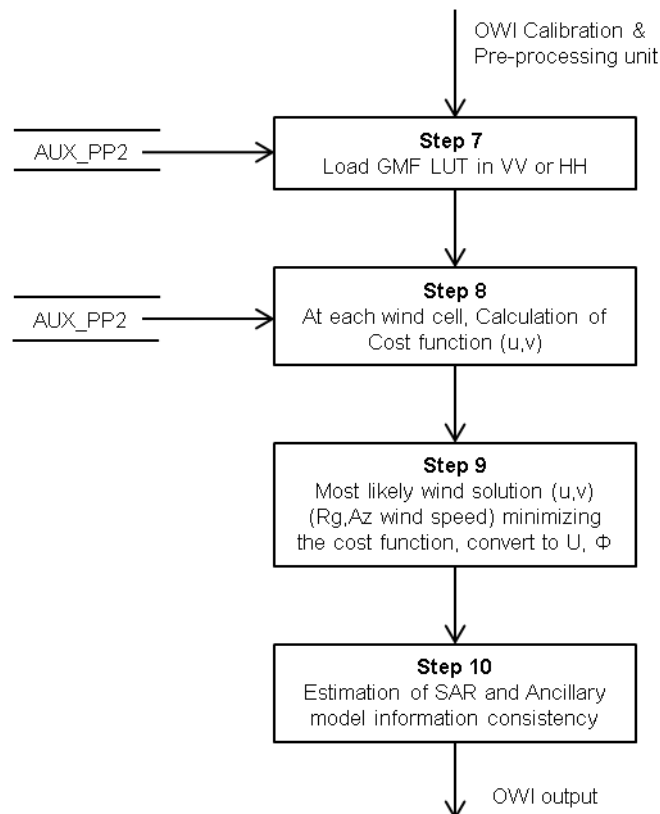


Figure 5-6 Inversion Unit Flowchart (after IPF 3.10)

5.3.2 Function and Purpose

At this level, the parameters of the wind vector are estimated using statistical Bayesian inversion. The different processing steps in the flowchart are described below.

Step 7: Load GMF LUT in VV or HH

This step aims to load the GMF LUT as respect to the GMF and polarization ratio specified in the AUX_PP2.

Input parameters:

θ_{LUT} : The incidence angle for the GMF LUT (inspace vector space rate 0.1deg)

φ_{LUT}	: The wind direction relative to the sensor range axis for GMF LUT (inspace vectors space rate 1 deg)
V_{LUT}	: The wind speed (inspace vectors space rate 0.2m/s)

Output parameters:

$\sigma_{LUT}^0(\theta_{LUT}, \varphi_{LUT}, V_{LUT})$: Equivalent NRCS GMF LUT in VV or HH in dB

Procedure:

The GMF LUT gives:

$$\sigma_{LUT}^0 = \begin{cases} \text{GMF}_{VV}(\theta_{LUT}, \varphi_{LUT}, V_{LUT}) & , \text{ if VV} \\ \text{GMF}_{HH}(\theta_{LUT}, \varphi_{LUT}, V_{LUT}) \cdot \text{PR}(\theta_{LUT}, \varphi_{LUT}) & , \text{ if HH} \end{cases} \quad (31)$$

Where GMF_{VV} and GMF_{HH} and PR are specified by the AUX_PP2; in case of GMF_{HH} is not specified by the AUX_PP2 $\text{GMF}_{HH} = \text{GMF}_{VV}$. Details about the polarization ratio can be found in section Appendix A 6

Step 8: Estimate the cost function at each wind cell

For each grid cell of the OWI grid, the cost function is calculated.

Input parameters:

$\{\theta_i\}_{i \in \mathcal{G}_{\text{SAR Wind}}}$: The incidence angle at each SAR wind cell from step 3
$\{(U_{AP}, \varphi_{AP})_i\}_{i \in \mathcal{G}_{\text{SAR Wind}}}$: The ancillary wind speed and (corrected) wind direction w.r.t. radar looking direction re-sampled on SAR wind grid $\mathcal{G}_{\text{SAR wind}}$ from step 5
$\{(\sigma^0)_i\}_{i \in \mathcal{G}_{\text{SAR Wind}}}$: NRCS estimated at each SAR wind cell from step 7 in dB
$\sigma_{LUT}^0(\theta_i, \varphi_{LUT}, V_{LUT})$: Equivalent NRCS GMF LUT in VV or HH at the closest incidence angle in dB

Output parameters:

$\mathbf{u}_{LUT}, \mathbf{v}_{LUT}$: As respectively relative wind speed on Range and Azimuth direction
$\{(u_{AP}, v_{AP})_i\}_{i \in \mathcal{G}_{\text{SAR Wind}}}$: As respectively relative wind speed on Range and Azimuth direction given by the model at the given wind cell
$\{F_{\text{cost}}(\mathbf{u}_{LUT}, \mathbf{v}_{LUT})_i\}_{i \in \mathcal{G}_{\text{SAR Wind}}}$: Estimation of the cost function of the wind cell element

Procedure:

As respective relative wind speed on Range and Azimuth direction the u and v are given by:

$$\begin{cases} \mathbf{u}_{LUT} = V_{LUT} \cos(\varphi_{LUT}) \\ \mathbf{v}_{LUT} = V_{LUT} \sin(\varphi_{LUT}) \end{cases} \quad (32)$$

And:

$$\{(u_{AP}, v_{AP})_i\}_{i \in \mathcal{G}_{SAR\ Wind}} = \{(U_{AP} \cos \varphi_{AP}, U_{AP} \sin \varphi_{AP})_i\}_{i \in \mathcal{G}_{SAR\ Wind}} \quad (33)$$

For each wind cell of the OWI grid, the cost function is given by:

$$F_{cost}(\mathbf{u}_{LUT}, \mathbf{v}_{LUT})_i = \left(\frac{\mathbf{u}_{LUT} - u_{AP}}{\delta_u} \right)^2 + \left(\frac{\mathbf{v}_{LUT} - v_{AP}}{\delta_v} \right)^2 + \left(\frac{\sigma_{LUT}^0(\theta_i, \varphi_{LUT}, V_{LUT}) - \sigma_i^0}{\delta_\sigma} \right)^2 \quad (34)$$

Where the variability δ_u , δ_v and δ_{sigma} is given by the PP2. Default values are 2m/s, 2m/s and 0.1dB

Step 9: Find the most likely solution

By minimizing over the LUT the cost function, the most likely solution \mathbf{u}, \mathbf{v} is found for each wind cell i and transform to $\{(U, \varphi)\}_{i \in \mathcal{G}_{SAR\ Wind}}$

Input parameters:

$\{F_{cost}(\mathbf{u}_{LUT}, \mathbf{v}_{LUT})_i\}_{i \in \mathcal{G}_{SAR\ Wind}}$: Estimation of the cost function of the wind cell element

Output parameters:

$\{(\mathbf{u}, \mathbf{v})_i\}_{i \in \mathcal{G}_{SAR\ Wind}}$: Couple u, v on the LUT minimizing the cost function model at the given wind cell

$\{(U, \varphi)\}_{i \in \mathcal{G}_{SAR\ Wind}}$: Corresponding wind speed and direction.

Procedure:

At each wind cell of the OWI grid, the couple u, v is found by minimizing the cost function. The couple u, v is transformed to get U, φ the wind speed and direction as respect to the sensor geometry. The wind direction is then converted has the direction from which the wind blows as respect to the North

$$(\mathbf{u}, \mathbf{v}) = \operatorname{argmin}_{(u, v) \in (\mathbf{u}_{LUT}, \mathbf{v}_{LUT})} (F_{cost}(\mathbf{u}_{LUT}, \mathbf{v}_{LUT})) \quad (35)$$

Step 10: Inversion quality flag

This step aims at evaluating the consistency between the NRCS as measured by the SAR and the a priori wind information for each wind cell for the OWI grid, and remains unchanged compare to previous OWI inversion Unit. Please refer to step 11 in section 5.2.

This section presents an overview of the input files used by the OWI algorithm. The complete format specification is provided:

- in document A-16 for the auxiliary files,
- in document A-14 for the Sentinel-1 SAR products,
- in document A-12 for the job order.

6.1 Auxiliary Data Files

Auxiliary data are divided into two categories:

- Internal files: They are part of the processor as they do not change with time. They are stored locally.
- External files: They contain information which may vary from one processing to another.

6.1.1 Internal Auxiliary Data Files

6.1.1.1 Coastline and Land Masking Data

Wind inversion processing is not performed if land coverage is greater than 10% in the imagette considered. The land coverage is estimated as the ratio between the surface area of imagette and the surface area of a local land mask that covers the imagette.

The accuracy of the coastline and land masking depends on the accuracy of the reference coastline/landmask effectively used.

Details of the Coastline and Land Masking data are provided in A-16.

The GSHHS coastline is used. This shoreline database is available at <http://www.ngdc.noaa.gov/mgg/shorelines/gshhs.html>.

6.1.2 External Auxiliary Data Files

6.1.2.1 ECMWF Atmospheric Model

Meridional and zonal wind component at 10 m above the sea surface from the ECMWF atmospheric model is required with spatial and temporal resolution of at least 0.25 degrees every 3 hours (currently available). Recently, ECMWF announced that they will by the end of 2009 provide wind data on 0.125 degree horizontal grid.

Details of the ECMWF Atmospheric Model are provided in A-16.

6.1.2.2 Sea Ice Data

Wind inversion processing is not performed if sea ice coverage is greater than 10% in the imagette considered. This percentage is directly given by the sea ice concentration product delivered by the OSI SAF at a spatial resolution of 10 km every day. The product is available on the OSI SAF sea ice FTP server (<ftp://saf.met.no/prod/ice>) on HDF5 and GRIB format or on MERSEA server (<http://mersea.met.no>).

Details of the Sea Ice Data are provided in A-16.

6.1.2.3 L2 Processor Parameters Auxiliary Data

Table 6-1 lists the auxiliary processing parameters used by the OWI processing algorithm described in this document. The names in the “Parameter” column represent the parameter names used in this document. The parameter names in the auxiliary processing parameter files are described in Table 6-1.

Table 6-1 Processor Parameters Auxiliary data list for OWI

Parameter	Description	Unit	Default value
<i>cell_size</i>	Size of the SAR derived wind field	m	1000
<i>dist2shore_km</i>	Distance to shore where the processing is not performed	Km	2
<i>stdev_speed</i>	Standard deviation error of the wind speed provided by ancillary wind information	m/s	2
<i>stdev_dir</i>	Standard deviation error of the wind direction provided by ancillary wind information	Degree	20
<i>Gmf_index</i>	Name of the GMF to be used for wind inversion	-	CMOD-IFR2
<i>Threshold_Qflag_inversion</i>	Value above which minimization in the inversion is considered as low quality	-	TBD
<i>Threshold_Qflag_Kc</i>	Value above which the calibration of the product is considered as badly calibrated	-	TBD
<i>Threshold_Pb</i>	Value above which the NRCS estimated at the SAR wind cell resolution is considered as low quality	-	TBD
<i>Pfa</i>	Probability of false alarm for the detection of bright target.	-	10 ⁻⁷

6.2 SAR Product

6.2.1 SAR Image

Table 6-2 presents the L1 product characteristics accepted by the L2 OCN processor. For SM and TOPS (IW, EW) modes, the input to the OWI algorithm is an internal GRD product with the following characteristics:

- Ground range projected
- Range and Azimuth matched filter windows applied
- Azimuth antenna pattern corrections applied
- Range spreading loss correction applied
- Elevation antenna pattern correction applied
- Single look in range and azimuth
- 16-bit integer per pixel

The OWI algorithm does not need the phase information from the L1 SLC product. Therefore, it is more effective to generate the GRD product in the L1 processor including combining all the individual bursts in the TOPS modes.

For WV mode the input to the L2 processor is an internal SLC product with the following characteristics:

- Slant range
- Range and Azimuth matched filter windows not applied
- Azimuth antenna pattern corrections not applied
- Range spreading loss correction applied
- Elevation antenna pattern correction applied
- Single look in range and azimuth
- 32-bit float real part and 32-bit float imaginary part per pixel

Table 6-2 also shows that the L2 processor can process L1 ASAR data. This ASAR data processing is supported in the Test mode where the L2 processor is controlled through command line.

Table 6-2 L2 Processing Support vs Input L1 Product Characteristics

Sensor	Input L1 Product			Supported L2 Processing			
	Product Type	Acq. Mode		Ocean Swell Spectra (OSW)	Ocean Wind Field (OWI)	Radial Surface Velocity (RVL)	Doppler Grid
	For OWI	For OSW and RVL					
Sentinel-1	GRD	SLC	SM	✓	✓	✓	✓
Sentinel-1	GRD	SLC	IW		✓	✓	✓
Sentinel-1	GRD	SLC	EW		✓	✓	✓
Sentinel-1		SLC	WV	✓	✓	✓	✓
ASAR	GRD	SLC	IM	✓	✓	✓	✓
ASAR		SLC	WV	✓	✓	✓	✓

6.2.2 SAR Product Annotation

These are the variables read in the step of the calibration and process unit. They are defined in A-14.

L_x^l, L_y^l :	Number of range and azimuth pixels in the level-1 image.
P_x^l, P_y^l :	Image pixel size in meters in range and azimuth direction.
$\{(x, y)_i\}_{i \in \mathcal{G}_{LADS}}$	Arrays of index tie points given by the geo-Location grid ADS
$\{lon_i, lat_i\}_{i \in \mathcal{G}_{LADS}}$:	Arrays of longitude and latitudes at tie points $\{(x, y)_i\}_{i \in \mathcal{G}_{LADS}}$
$\{t_i\}_{i \in \mathcal{G}_{LADS}}$:	Array of two-way slant range times at tie points $\{(x, y)_i\}_{i \in \mathcal{G}_{LADS}}$
$\{\theta_i\}_{i \in \mathcal{G}_{LADS}}$:	Array of incidence angles at tie points $\{(x, y)_i\}_{i \in \mathcal{G}_{LADS}}$
K^c :	The calibration vector, LUT
P_{TXRX}^{ol} :	The Transmitter/Receiver polarization.
Φ :	The satellite ground track direction.
F^{srg} :	Flag set to 1 if slant-range-to-ground-range conversion is applied.
T_0 :	UTC time of first pixel of first line (early azimuth).
θ_c :	The incidence angle at swath centre
R^A :	The aspect ratio
P_x^G, P_y^G :	Ground pixel size corrected for aspect ratio
l :	The input image ($L_x \times L_y$) to compute Amplitude for NRCS calculation

6.3 Internal Input Parameters

6.3.1 Job Order

This file contains all the fields required to define a single S-1 data processing job (e.g. list of files names and path to be used for processing). A detailed description of the Job Order is provided in document A-12.

6.3.2 Processor Configuration File

This file contains the names of files that exist locally on the processor workstation that are required as input to the L2 Processor. A detailed description of the Processor Configuration File is provided in document A-12.

6.3.3 PRM_LOPin

Additional file to store internal processing parameters for the L2 Processor, including the OWI component (parameters TBD).

7 List of Symbols

The following symbols are used by the wind retrieval algorithm.

Table 7-1 Variables Used by the Wind Retrieval Algorithm

Variable	Description	Unit
L_x^I, L_y^I	Number of range and azimuth pixels in the level-1 image	samples
P_x^I, P_y^I	Image pixel size in meters in range and azimuth direction	m
$\{(x, y)_i\}_{i \in \mathcal{G}_{LADS}}$	Arrays (M,N) of index tie points given by the geo-Location grid ADS	samples
$\{lon_i, lat_i\}_{i \in \mathcal{G}_{LADS}}$	Arrays (M,N) of longitude and latitudes at tie points $\{(x, y)_i\}_{i \in \mathcal{G}_{LADS}}$	degree
$\{t_i\}_{i \in \mathcal{G}_{LADS}}$	Array (M,N) of two-way slant range times at tie points $\{(x, y)_i\}_{i \in \mathcal{G}_{LADS}}$	s
$\{\theta_i\}_{i \in \mathcal{G}_{LADS}}$	Array (M,N) of incidence angles at tie points $\{(x, y)_i\}_{i \in \mathcal{G}_{LADS}}$	degree
K^c	Calibration constant	-
K_{GeoCal}^I	Geophysical Calibration constant	-
$Q_{K_{GeoCal}^c}^{flag}$	Calibration constant flag	boolean
<i>Threshold_Qflag_Kc</i>	Threshold for the calibration constant	-
P_{TXRX}^{ol}	Transmitter/Receiver Polarization	
Φ	The satellite ground track direction	degree
F^{srg}	The Slant range to Ground range conversion flag	boolean
T_0	UTC time of first pixel of first line (early azimuth)	UTC
θ_c	Incidence angle at swath centre	degree
R^A	Aspect ratio	-
P_x^G, P_y^G	Image Ground pixel size corrected for aspect ratio	m
P^W	The expected wind cell size	m
S^f	The sampling factor (to determine the number of SAR pixels to be averaged)	-
P_x^W, P_y^W	Wind cell size in meters in range and azimuth directions	m
L_x^W, L_y^W	Number of range and azimuth wind cells in the SAR derived wind field	samples
$\{(x, y)_i\}_{i \in \mathcal{G}_{SAR\ Wind}}$	The index values corresponding to the centre of SAR derived wind cells	samples

Variable	Description	Unit
$\{lon_i, lat_i\}_{i \in \mathcal{G}_{SAR\ Wind}}$	The set of longitudes and latitudes at each SAR wind cell	degree
$\{(DN^I)_i\}_{i \in \mathcal{G}_{SAR\ Image}}$	Digital number at each SAR image pixels	-
$\{(A^I)_i\}_{i \in \mathcal{G}_{SAR\ Image}}$	Signal amplitude at each SAR image pixels	-
$\{(A^W)_i\}_{i \in \mathcal{G}_{SAR\ Wind}}$	The averaged amplitude at each SAR wind cell	-
$\{(B^I)_i\}_{i \in \mathcal{G}_{SAR\ Image}}$	Mask array of bright targets detected at each SAR image pixels	boolean
$\{(B^W)_i\}_{i \in \mathcal{G}_{SAR\ Wind}}$	Array of percentage of bright targets detected in the SAR image pixels used for the computation of SAR wind pixel $\{(x, y)_i\}_{i \in \mathcal{G}_{SAR\ Wind}}$	-
<i>Threshold_Pb</i>	Threshold limit for the percentage of bright targets detected in the SAR image pixels used for the computation of SAR wind pixel above which the NRCS computed is considered as optimal but could be significantly different from the nominal	-
<i>pfa</i>	Probability of false alarm for the detection of bright target.	-
$\{t_i\}_{i \in \mathcal{G}_{SAR\ Wind}}$	The two-way slant range times at each SAR wind cell	s
$\{\theta_i\}_{i \in \mathcal{G}_{SAR\ Wind}}$	The incidence angle at each SAR wind cell	degree
$\{(lutsigma0)_i\}_{i \in \mathcal{G}_{SAR\ Wind}}$	Radar cross section calibration LUT value estimated at each center of SAR wind cell	-
$\{(lutBeta0)_i\}_{i \in \mathcal{G}_{SAR\ Wind}}$	Radar brightness calibration LUT value estimated at each center of SAR wind cell	-
b	scaling factor given in the calibration LUT	-
$\{(\sigma^0)_i\}_{i \in \mathcal{G}_{SAR\ Wind}}$	The normalised radar cross section (NRCS) at each SAR wind cell	-
$\{(M^W)_i\}_{i \in \mathcal{G}_{SAR\ Wind}}$	Mask array containing land flag at each SAR wind cell	boolean
$\{(lon_{AP})_i, (lat_{AP})_i\}_{i \in \mathcal{G}_{A\ Priori}}$	Longitude and latitude values of ancillary wind information points	degree
$\{(u_{AP})_i, (v_{AP})_i\}_{i \in \mathcal{G}_{A\ Priori}}$	Zonal and meridional components of ancillary wind vectors	m/s
$\{(l_{AP})_i\}_{i \in \mathcal{G}_{A\ Priori}}$	Ice mask	boolean
$\{(U_{AP})_i\}_{i \in \mathcal{G}_{SAR\ Wind}}$	The ancillary wind speed re-sampled on SAR wind grid	m/s
$\{(\varphi_{AP})_i\}_{i \in \mathcal{G}_{SAR\ Wind}}$	The ancillary wind direction re-sampled on SAR wind grid	degree
$\{(\phi_{AP})_i\}_{i \in \mathcal{G}_{SAR\ Wind}}$	The ancillary wind direction with respect to the line-of sight direction of the SAR antenna	degree
$\{U_i\}_{i \in \mathcal{G}_{SAR\ Wind}}$	The estimated SAR wind speed values	m/s

Variable	Description	Unit
$\{\varphi_i\}_{i \in \mathcal{G}_{\text{SAR Wind}}}$	The estimated SAR wind direction values	degree
$\{(Q_{inversion})_i\}_{i \in \mathcal{G}_{\text{SAR Wind}}}$	Flag for consistency between ancillary model output and NRCS used in the wind inversion scheme	boolean
<i>Threshold_Qflag_inversion</i>	Threshold limit above which the consistency between ancillary model output and NRCS used in the wind inversion scheme is considered as low.	-
$\{(Q_{wind}^{flag})_i\}_{i \in \mathcal{G}_{\text{SAR Wind}}}$	Flag for SAR wind quality flag at each SAR wind cell	boolean

8 OWI Output Component annotations

The following is a brief overview OWI component annotations in the L2 OCN product NetCDF file. The complete, detailed L2 product format is described in A-14.

The L2 OCN annotations data set includes the following dimensions

- Number of wind cells in the range direction
- Number of wind cells in the azimuth direction

The L2 OCN data set also includes the following variables per wind cell:

- Longitude/latitude at cell centre
- Two way slant range time at cell centre, only before IPF version 2.82 included
- Zero Doppler time at cell centre, only before IPF version 2.82 included
- Incidence angle at cell centre (in range), reported for each azimuth line in the cell
- Satellite heading
- Normalised radar cross section for each SAR wind cell and for each polarization.
- Percentage of bright targets detected in each SAR wind cell and removed for the computation of the NRCS in co-polarization
- Predicted NRCS in co-polarization from CMOD (and polarization ratio for HH co-polarization) and ECMWF a priori 10m wind for each SAR wind cell.
- Geophysical calibration constant vector for each L2 OCN product
- Calibration quality flag for each L2 OCN product
- SAR wind speed and direction for each SAR wind cell
- Inversion quality indicator for each SAR wind cell
- SAR wind quality flag for each SAR wind cell
- Auxiliary Data Derived Statistics
 - ECMWF a priori 10m height wind speed for each SAR wind cell
 - ECMWF a priori 10m height wind direction for each SAR wind cell
 - Land flag for each SAR wind cell
 - Percentage of land coverage (for SM in coastal zones) for each SAR wind cell
 - Ice flag for each SAR wind cell
- Variables from RVL and OSW components
 - Radial velocities (interpolated) for each SAR wind cell
 - Dominant wavelength of two most energetic wave partitions (interpolated) for each SAR wind cell (except for TOPS)
 - Dominant wave direction of two most energetic wave partitions (interpolated) for each SAR wind cell (except for TOPS)
 - SAR significant waveheight of two most energetic wave partitions (interpolated) for each SAR wind cell (except for TOPS)
 - Significant waveheight for the wind sea part of the total wave height spectrum (interpolated) for each SAR wind cell (except for TOPS)

MPC-0469

The L2 OCN data set includes the global attributes:

- Title/description of L2 OCN product
- Level 1 source product name
- Mission name
- Mission phase
- Polarisation
- Acquisition station
- OSW algorithm version
- OWI algorithm version
- RVL algorithm version
- IDL version (obsolete after IPF version 2.84)
- IPF version
- Geophysical model function used for OWI processing
- Polarisation ratio model used for OWI processing
- Contact information
- Processing start time
- Processing centre
- First measurement time
- Last measurement time
- Coastline, wind, ice, bathymetry, stokes and land masking auxiliary data source
- OWI noise correction flag value

Appendix A 1 -FORMAT_ANGLE

This routine performs modulo operation on input *angle* given the value of *cycle*. The output value is then either formatted between 0 and *cycle* (when COMPASS_FORMAT keyword is set) or between $-cycle/2$ and $+cycle/2$. IDL language was used until IPF 2.82, after with IPF 2.84 and later the LOP is coded using Python.

Syntax:

```
IDL>Result=FORMAT_ANGLE(Angle, COMPASS_FORMAT=compass_format,
CYCLE=cycle) (36)
```

Arguments:

Angle: The angle to be formatted (expressed in degrees)

Keywords:

COMPASS_FORMAT: If set to 1, then the output value will be formatted between 0 and *cycle*, else it will be between $-cycle/2$ and $cycle/2$

CYCLE: The modulo value (set to 360° if not defined)

Procedure:

1. The *Angle* value is transformed as follows:

$$Angle = Angle \text{ mod } cycle \quad (37)$$

$$Angle = \begin{cases} Angle + cycle & \text{if } angle < -cycle/2 \\ Angle - cycle & \text{if } angle > +cycle/2 \end{cases} \quad (38)$$

2. Finally, The returned value of *Angle* is given by:

$$Angle = \begin{cases} Angle + cycle & \text{if } COMPASS_FORMAT=1 \\ Angle - cycle & \text{else} \end{cases} \quad (39)$$

This IDL procedure constructs a Delaunay triangulation of a planar set of points. After the irregularly gridded data points have been triangulated, the function TRIGRID is invoked to interpolate surface values to a regular grid. *IDL language was used until IPF 2.82..*

Syntax:

```
IDL > TRIANGULATE, X, Y, triangles, boudaryPts (40)
```

Arguments:

<i>X</i> :	An array that contains the X coordinates of the points to be triangulated.
<i>Y</i> :	An array that contains the Y coordinates of the points to be triangulated.
<i>triangles</i> :	A named variable that, on exit, contains the list of triangles in the Delaunay triangulation of the points specified by the X and Y arguments.
<i>boundaryPts</i> :	An optional, named variable that, upon return, contains a list of the indices of the boundary points in counter-clockwise order

After IPF2.8x and later, the LOP is coded using Python, the interpolation methods have been replaced based on GDAL interpolation methods.

Appendix A 3 -TRIGRID - Interpolation from Triangulation

This IDL function returns a regular grid of interpolated Z values given data points defined by the parameters X, Y, and Z and a triangulation of the planar set of points determined by X and Y. Extrapolation for grid points outside of the triangulation area is also an option. An input triangulation can be constructed using the procedure [TRIANGULATE](#). *IDL language was used until IPF 2.82 included..*

Syntax:

```
IDL> result =TRIGRID(X,Y,Z,triangles,GS,limits,/QUINTIC,EXTRAPOLATE =
b,XGRID = xg,YGRID = yg)      (41)
```

Arguments:

- X, Y, Z:** Input arrays of X, Y, and Z coordinates of data points. All three arrays must have the same number of elements.
- triangles:** A longword array of the form output by the IDL TRIANGULATE function. That is, Triangles has the dimensions (3, number of triangles) and, for each i, *triangles*[0, i], *triangles*[1, i] and *triangles*[2, i] are the indices of the vertices of the i-th triangle
- GS:** If present, GS should be a two-element vector [XS, YS], where XS is the horizontal spacing between grid points and YS is the vertical spacing.
- limits:** If present, Limits should be a four-element vector [x0, y0, x1, y1] that specifies the data range to be gridded (x0 and y0 are the lower X and Y data limits, and x1 and y1 are the upper limits).

Keywords:

- EXTRAPOLATE:** Set this keyword equal to an array of boundary node indices (as returned by the optional parameter *b* of the TRIANGULATE procedure) to extrapolate to grid points outside the triangulation. Setting this keyword sets the quintic interpolation mode, as if the QUINTIC keyword has been specified
- QUINTIC:** If QUINTIC is set, smooth interpolation is performed using Akima's quintic polynomials from "A Method of Bivariate Interpolation and Smooth Surface Fitting for Irregularly Distributed Data Points" in ACM Transactions on Mathematical Software, 4, 148-159. For non-spherical data, the default method is linear interpolation. Derivatives are estimated by Renka's global method in "A Triangle-Based C1 Interpolation Method" in Rocky Mountain Journal of Mathematics, vol. 14, no. 1, 1984. Setting the EXTRAPOLATE

keyword implies the use of quintic interpolation; it is not necessary to specify both

XGRID: Set this keyword to a named variable that will contain a vector of X values for the output grid

YGRID: Set this keyword to a named variable that will contain a vector of Y values for the output grid

In IPF 2.8x and later, the LOP is coded using Python, the interpolation methods have been replaced based on GDAL interpolation methods

Appendix A 4 -INTERPOL - Linear 1D Interpolation

The IDL function performs linear, quadratic, or spline, interpolation on vectors with a regular or irregular grid. *IDL language was used until IPF 2.82 included.*

Syntax:

$$\text{IDL} > \text{Result} = \text{INTERPOL}(V, X, U) \quad (42)$$

Arguments

<i>V</i> :	An input vector of any type except string
<i>X</i> :	The abscissa values for <i>V</i> . <i>X</i> must have the same number of elements as <i>V</i> , and the values must be strictly ascending or descending
<i>U</i> :	The abscissa values for the result. The result will have the same number of elements as <i>U</i> .

In IPF 2.8x and later, the LOP is coded using Python, this interpolation method has been replaced based on `scipy.interpolate` interpolation method: `interp1d`

Appendix A 5 -BILINEAR - Bilinear Interpolation

This IDL function uses a bilinear interpolation algorithm to compute the value of a data array at each of a set of subscript values. This function returns a two-dimensional interpolated array of the same type as the input array. *IDL language is used until IPF 2.82 included.*

Syntax:
$$\text{IDL} > \text{Result} = \text{BILINEAR}(P, JX, JY) \quad (43)$$
Arguments:

P: A two-dimensional data array.

JX, JY: Arrays containing the X and Y "virtual subscripts" of P for which to interpolate values

After IPF 2.8x and later, the LOP is coded using Python, the bilinear interpolation method has been replaced based on scipy.interpolate interpolation methods: bisplrep/bisplev, interp2d, LinearNDInterpolator.

Appendix A 6 -POLARIZATION_RATIO

This function returns the polarization ratio as a function of the local incidence angle and the direction from which the wind is blowing with respect to the looking direction of the antenna. *IDL language is used until IPF 2.82.. In IPF 2.84 and later, the LOP is coded using Python, an equivalent function is also present.* In practice the polarization ratio is integrated to the GMF LUT for IPF 3.1x and later, to get the GMF LUT in HH.

The polarization ratio is triggered by the AUX_PP2.

Syntax:

$$IDL> Result = POLARIZATION_RATIO(\theta, \varphi, MODEL=model) \quad (44)$$

Arguments:

- θ : The local incidence angle.
- ϕ : The direction from which the wind is blowing with respect to the looking direction of the antenna

Keywords:

- MODEL: The selection of different polarization ratio models A-19A-21 can be done through this keyword

Procedure:

1. The polarisation ratio is given by:

$$PR = \begin{cases} \frac{(1+2 \tan^2 \theta)^2}{(1+0.7 \tan^2 \theta)^2}, & \text{if MODEL} = 0 \\ \frac{(1+2 \tan^2 \theta)^2}{(1+2 \sin^2 \theta)^2}, & \text{if MODEL} = 1 \\ PR_1^{\text{Mouche}}(\theta, \varphi), & \text{if MODEL} = 2 \\ PR_2^{\text{Mouche}}(\theta), & \text{if MODEL} = 3 \end{cases} \quad (45)$$

2. The wind dependent polarization ratio model proposed by Mouche et al A-19 is given by:

$$PR_1^{\text{Mouche}}(\theta, \phi) = C_0^\theta + C_1^\theta \cos(\phi) + C_2^\theta \cos(2\phi) \quad (46)$$

Where:

$$C_0^\theta = (P_0^\theta + P_\pi^\theta + 2P_{\pi/2}^\theta) / 4$$

$$C_1^\theta = (P_0^\theta - P_\pi^\theta) / 2$$

$$C_2^\theta = (P_0^\theta + P_\pi^\theta - 2P_{\pi/2}^\theta) / 4$$

With:

$$\begin{cases} P_0^\theta = 0.00650704 \cdot \exp(0.128983 \cdot \theta) + 0.992839 \\ P_{\frac{\pi}{2}}^\theta = 0.00782194 \cdot \exp(0.121405 \cdot \theta) + 0.992839 \\ P_\pi^\theta = 0.00598416 \cdot \exp(0.140952 \cdot \theta) + 0.992885 \end{cases}$$

3. The second polarization ratio model proposed by Mouche et al A-19 is given by:

$$P_2^{\text{Mouche}} = 0.00799793 \cdot \exp(0.125465 \cdot \theta) + 0.997379 \quad (47)$$

Appendix A 7 -LOGSIG - Log-Sigmoid Transfer Function

This function takes the input, which may have any value between plus and minus infinity and squashes the output between 0 and 1. This function is part of the `cmod_ifremer_inverse_vect.pro` IDL function presented in Appendix A 8 -. *IDL language is used until IPF 2.82. In IPF 2.84 and later, the LOP is coded using Python, an equivalent function is also present.* In practice, the direct inverse of the Cmod GMF is not used anymore after IPF 3.1x and later, on which the wind inversion relies on GMF LUT.

Figure 8-1 Log-Sigmoid Transfer Function

Syntax:

$$\text{IDL}>\text{Result} = \text{LOGSIG}(X) \quad (48)$$

Arguments:

X: Scalar or array of values

Procedure:

1. The output of the log-Sigmoid function is given by:

$$\text{Result} = \frac{1}{1+\exp(-X)} \quad (49)$$

Appendix A 8 -CMOD_IFREMER_INVERSE_VECT

This function returns the neutral equivalent wind speed at 10 meters as a function of incidence angle, linear NRCS in VV-polarisation, and the direction from which the wind is blowing with respect to the radar line-of-sight direction.

This corresponds to the neural network implementation of the CMOD-IFR2 A-20. .

IDL language is used until IPF 2.782. In IPF 2.84 and later, the LOP is coded using Python, an equivalent function is also present. In practice, the direct inverse of the Cmod GMF is not used anymore after IPF 3.1x and later, on which the wind inversion relies on GMF LUT.

The proposed architecture is presented in Figure 8-2.

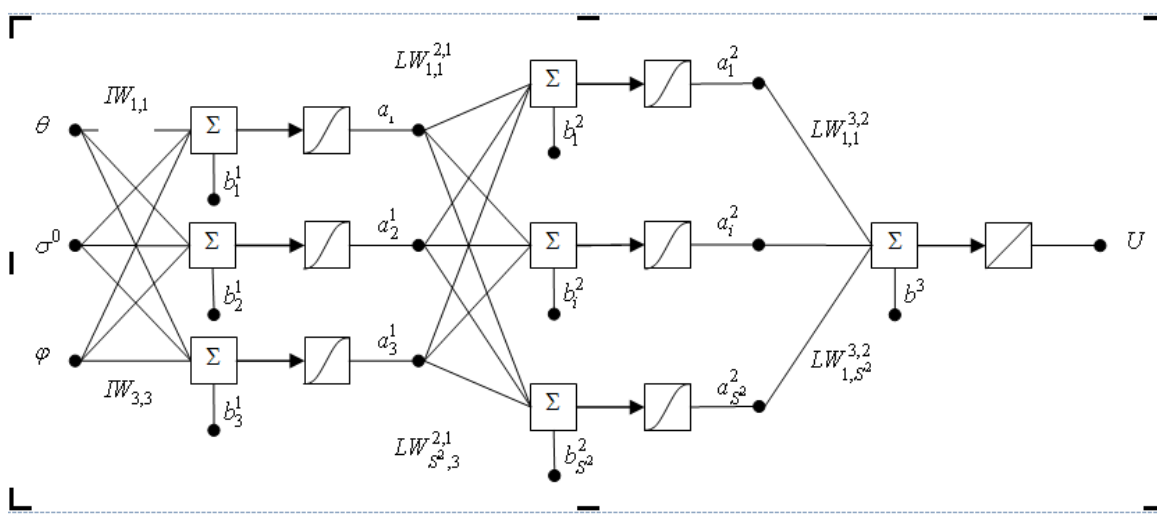


Figure 8-2 Neural Network Architecture for the Implementation of the Inverse CMOD Scattering Models

Syntax:

IDL>Result = CMOD_IFREMER_INVERSE_VECT(θ , σ^0 , ϕ , CMOD_MODEL=cmod_model) (50)

Arguments:

- θ : The local incidence angle (can be a scalar or an array)
- σ^0 : The NRCS value expressed in linear scale. The NRCS value is assumed to correspond to signal backscattered from the sea surface after transmission and reception in vertical polarization (Must have the same size than θ).
- ϕ : The direction from which the wind is blowing with respect to the looking direction of the antenna (Must have the same size than θ).

Keywords:

CMOD_MODEL: The selection of two different scattering models developed by IFREMER can be done through this keyword:

- ‘CMOD-IFR2 NN’ A-20 (default)

Procedure

1. The linear NRCS value will first be expressed in dB:

$$\sigma_{\text{dB}}^0 = 10 \cdot \log_{10}(\sigma^0) \quad (51)$$

2. The wind speed is given by:

$$U = LW^{3,2} \# \text{logsig}(LW^{2,1} \# [\text{logsig}(IW \# P + B^1)] + B^2) + B^3, \quad (52)$$

Where:

$$P = [\theta, \sigma^0, \varphi]$$

denotes the matrix multiplication operator.

3. The values of arrays B^1 , B^2 , B^3 , $LW^{3,2}$ and matrices $IW, LW^{2,1}$ for the CMOD-IFR2 inverse model A-20 are given hereafter (\$ means that the line is not finished).

```
B1 = [      2.082886, $
      -0.841942, $
      -0.656464]
```

```
B2 = [  -70.326805, $
      -19.754431, $
         67.888680, $
         10.133004, $
      -128.439680, $
      -89.573363, $
         69.218988, $
         65.189747, $
         73.432775, $
      -94.562285, $
      -67.835318, $
         26.419743, $
      -52.157728, $
         81.903807, $
      -37.509473, $
      -73.216408, $
         64.222839, $
         24.666035, $
      -80.372419, $
      -89.579006, $
      -78.090509, $
         27.960399, $
         57.385043, $
```

-75.883218, \$
 -50.199558, \$
 59.060482, \$
 -93.676147, \$
 -24.395929, \$
 65.428578, \$
 28.466197, \$
 40.064443, \$
 -4.722488, \$
 -135.604384, \$
 -15.183091, \$
 13.412278]

B3 = [39.969936]

IW1 = [[-0.010157, -0.038371, -0.034955], \$
 [0.003006, 0.054323, -0.003453], \$
 [0.154295, 0.071817, 0.000140]]

LW21 = [[2.300742, 49.041606, 65.611377], \$
 [-4.807824, -0.882009, 21.627157], \$
 [2.474316, -40.430879, -64.933850], \$
 [-5.145791, -9.558264, 14.360309], \$
 [3.104158, 38.846043, 121.278273], \$
 [-0.179018, 3.900986, 85.507900], \$
 [1.989728, -37.182961, -66.626101], \$
 [16.412028, -52.423042, -55.026843], \$
 [5.607228, -53.500970, -70.431265], \$
 [-17.480667, 67.298780, 90.331722], \$
 [-3.804436, 45.836751, 64.684127], \$
 [-0.107370, -26.368820, -21.066112], \$
 [-15.385189, 66.336720, 60.627566], \$
 [11.013927, -64.134395, -69.747972], \$
 [-2.227543, 38.387985, 28.990207], \$
 [1.847110, 52.927378, 68.190684], \$
 [-5.872740, -44.349600, -57.595335], \$
 [-1.581706, -26.577835, -18.063290], \$
 [-18.123057, 80.806115, 70.988909], \$
 [4.398687, 76.879126, 79.315191], \$
 [4.178159, 63.939943, 69.415459], \$
 [1.593884, -24.605682, -24.212040], \$
 [11.370787, -65.499163, -48.275269], \$
 [4.839488, 58.663573, 67.409264], \$
 [-7.781707, 36.649118, 47.367479], \$
 [9.883707, -61.424425, -50.406215], \$
 [-17.044545, 64.785425, 89.740842], \$
 [-119.555883, 14.829578, 19.567950], \$



```

[      -5.072296,      -45.552059,      -59.392445], $
[       8.518015,      -10.877613,      -30.871287], $
[       6.261165,      -30.988114,      -36.863065], $
[      -5.047135,       12.180838,      -12.710277], $
[      -9.489117,       77.482996,      131.658583], $
[     -32.208368,        9.418533,       13.060133], $
[      16.925168,      -22.145650,      -11.276770] ]

```

```

LW32 = [      -74.671245, $
          -4.886914, $
        -141.271646, $
           39.275758, $
          -0.799615, $
           86.927814, $
           75.283134, $
          140.200911, $
          -23.311010, $
           41.046728, $
          -91.464701, $
          103.025508, $
            0.402924, $
        -142.039681, $
          -17.795908, $
           61.086801, $
           60.372377, $
          -33.978165, $
            5.748143, $
           32.880609, $
        -104.682748, $
        -113.455746, $
            22.218793, $
           66.169141, $
           46.710607, $
          -34.785100, $
          -42.544244, $
          162.762315, $
          -78.819174, $
          -3.078224, $
           84.885748, $
          -0.250489, $
            2.269681, $
          14.145298, $
            4.508966]

```

Appendix A 9 -CMOD_IFREMER

This function returns the linear NRCS in VV-pol as a function of incidence angle, neutral equivalent wind speed at 10 meters height, and the direction from which the wind is blowing with respect to the radar line-of-sight direction.

There are several CMOD-type functions available in the literature. The IPF used CMOD-IFR2 model A-20 by default until IPF 3.1. Please note that the choice of the GMF is triggered by the AUX_PP2.

IDL language is used until IPF 2.82. In IPF 2.84 and later, the LOP is coded using Python, an equivalent function is also present.

Syntax

```
IDL> Result =CMOD_IFREMER( $\theta$ ,  $U_{10}$ ,  $\phi$ , CMOD_MODEL =
cmod_model)      (53)
```

Arguments

θ :	The local incidence angle (can be a scalar or an array)
U_{10} :	The neutral equivalent wind speed at 10 meters height in [m/s] (must have the same size than θ).
ϕ :	The direction from which the wind is blowing with respect to the looking direction of the antenna (must have the same size than θ).

Keywords

CMOD_MODEL:	The selection of two different scattering models developed by IFREMER can be done through this keyword: <ul style="list-style-type: none"> ‘CMOD-IFR2’ A-20 (default)
-------------	--

Procedure

1. The linear NRCS for VV-pol is given by:

```
IDL> Result =CMOD_IFREMER( $\theta$ ,  $U_{10}$ ,  $\phi$ , CMOD_MODEL = cmod_model), (54)
```

2. Coefficient B0 is given by

$$B0 = 10.^{(\text{ALPH} + \text{BETA} * \text{sqrt}(U10))},$$

Where:

$$\text{ALPH} = C[1] + C[2] * P1 + C[3] * P2 + C[4] * P3$$

$$\text{BETA} = C[5] + C[6] * P1 + C[7] * P2$$

$$P1 = \theta_i$$

$$P2 = (3.*xSQ-1.)/2.$$

$$P3 = (5.*xSQ-3.)* \theta_i/2.$$

$$\theta_i = (\theta - 36.) / 19.$$

$$xSQ = \theta_i * \theta_i$$

3. CMOD-IFR2

Coefficient B1 is given by:

$$B1 = C[8] + C[9]*pv1 + (C[10]+C[11]*pv1)*pt1 + (C[12]+C[13]*pv1)*pt2,$$

Where:

$$pv0 = 1.$$

$$pv1 = vitnor$$

$$pv2 = 2*vitnor*pv1 - pv0$$

$$pv3 = 2*vitnor*pv2 - pv1$$

$$pt0 = 1.$$

$$pt1 = tetanor$$

$$pt2 = 2*tetanor*pt1 - pt0$$

$$pt3 = 2*tetanor*pt2 - pt1$$

Where:

$$tetanor = (2.*x - (tetamin+tetamax)) / (tetamax-tetamin)$$

$$vitnor = (2.*V - (vmax+vmin)) / (vmax-vmin)$$

$$tetamin = 18.$$

$$tetamax = 58.$$

$$vmin = 3.$$

$$vmax = 25.$$

Coefficient B2 is given by:

$$B2 = C[14] + C[15]*pt1 + C[16]*pt2 + (C[17]+C[18]*pt1+C[19]*pt2)*pv1 + (C[20]+C[21]*pt1+C[22]*pt2)*pv2 + (C[23]+C[24]*pt1+C[25]*pt2)*pv3$$

Where:

$$pv0 = 1.$$

$$pv1 = vitnor$$

$$pt0 = 1.$$

$$pt1 = tetanor$$

$$pv2 = 2*vitnor*pv1 - pv0$$

$$pv3 = 2*vitnor*pv2 - pv1$$

$$pt2 = 2*tetanor*pt1 - pt0$$

$$pt3 = 2*tetanor*pt2 - pt1$$

Where:

$$tetanor = (2.*x - (tetamin+tetamax)) / (tetamax-tetamin)$$

$$vitnor = (2.*V - (vmax+vmin)) / (vmax-vmin)$$

tetamin = 18.

tetamax = 58.

vmin = 3.

vmax = 25.

Coefficients C are given by

C[0] = 0.0

C[1] = -2.437597

C[2] = -1.5670307

C[3] = 0.3708242

C[4] = -0.040590

C[5] = 0.404678

C[6] = 0.188397

C[7] = -0.027262

C[8] = 0.064650

C[9] = 0.054500

C[10] = 0.086350

C[11] = 0.055100

C[12] = -0.058450

C[13] = -0.096100

C[14] = 0.412754

C[15] = 0.121785

C[16] = -0.024333

C[17] = 0.072163

C[18] = -0.062954

C[19] = 0.015958

C[20] = -0.069514

C[21] = -0.062945

C[22] = 0.035538

C[23] = 0.023049

C[24] = 0.074654

C[25] = -0.014713

Appendix A 10 - CMOD5n

This function returns the linear NRCS in VV-pol as a function of incidence angle, neutral equivalent wind speed at 10 meters height, and the direction from which the wind is blowing with respect to the radar line-of-sight direction.

Please note that the choice of the GMF is triggered by the AUX_PP2. Since IPF3.1x, Cmod5n is default GMF [A-25].

Syntax

$$Result = CMOD5n(\theta, U_{10}, \varphi) \quad (55)$$

Arguments

θ :	The local incidence angle
U_{10} :	The neutral equivalent wind speed at 10 meters height in [m/s].
φ :	The direction from which the wind is blowing with respect to the looking direction of the antenna.

Procedure

- The linear NRCS for VV-pol is given by:

$$Result = CMOD5n(\theta, U_{10}, \varphi), \quad (56)$$

- Coefficient B0 is given by

sig = B0 * (1.0 + B1 * CSFI + B2 * CS2FI) ** ZPOW Where:

$$B0 = (A3 ** GAM) * 10. ** (A0 + A1 * V)$$

$$V = U_{10}$$

$$CSFI = \cos(\varphi)$$

$$CS2FI = 2.00 * CSFI * CSFI - 1.00$$

$$ZPOW = 1.6$$

$$B1 = C[14] * V * (0.5 + X - \tanh(4. * (X + C[15] + C[16] * V)))$$

$$B1 = C[13] * (1. + X) - B1$$

$$B1 = B1 / (\exp(0.34 * (V - C[17])) + 1.)$$

$$B2 = (-D1 + D2 * V2) * \exp(-V2)$$

With

$$X = (\theta - THETM) / THETHR$$

$$THETM = 40.$$

```

THETR = 25.
XX = X * X
Y0 = C[18]
PN = C[19]
A = C[18] - (C[18] - 1.) / C[19]
B = 1. / (C[19] * (C[18] - 1.) ** (C[19] - 1.))
A0 = C[0] + C[1] * X + C[2] * XX + C[3] * X * XX
A1 = C[4] + C[5] * X
A2 = C[6] + C[7] * X
GAM = C[8] + C[9] * X + C[10] * XX
S0 = C[11] + C[12] * X
S = A2 * V
SS = S IF S >= S0
SS = S0 IF S < S0
A3 = 1 / (1 + EXP(-SS))
IF S < S0:
    A3 = A3 * (S / S0) ** (S0 * (1 - A3))
V0 = C[20] + C[21] * X + C[22] * XX
D1 = C[23] + C[24] * X + C[25] * XX
D2 = C[26] + C[27] * X
V2 = (V / V0 + 1.)
w1 = np.where(V2 < Y0)
IF V2 < Y0:
    V2 = A + B * (V2[w1] - 1.) ** PN
ALPH = C[1] + C[2] * P1 + C[3] * P2 + C[4] * P3
BETA = C[5] + C[6] * P1 + C[7] * P2
P1 =  $\theta_i$ 
P2 = (3.*xSQ-1.)/2.
P3 = (5.*xSQ-3.)*  $\theta_i$ /2.
 $\theta_i$  = ( $\theta$  - 36.)/19.
xSQ =  $\theta_i$  *  $\theta_i$ 

```

6. CMOD-IFR2

Coefficient B1 is given by:

$$B1 = C[8] + C[9]*pv1 + (C[10]+C[11]*pv1)*pt1 + (C[12]+C[13]*pv1)*pt2,$$

Where:

$$pv0 = 1.$$

$$\begin{aligned}
 pv1 &= vitnor \\
 pv2 &= 2*vitnor*pv1 - pv0 \\
 pv3 &= 2*vitnor*pv2 - pv1 \\
 pt0 &= 1. \\
 pt1 &= tetanor \\
 pt2 &= 2*tetanor*pt1 - pt0 \\
 pt3 &= 2*tetanor*pt2 - pt1
 \end{aligned}$$

Where:

$$\begin{aligned}
 tetanor &= (2.*x - (tetamin+tetamax))/(tetamax-tetamin) \\
 vitnor &= (2.*V - (vmax+vmin))/(vmax-vmin) \\
 tetamin &= 18. \\
 tetamax &= 58. \\
 vmin &= 3. \\
 vmax &= 25.
 \end{aligned}$$

Coefficient B2 is given by:

$$B2 = C[14] + C[15]*pt1 + C[16]*pt2 + (C[17]+C[18]*pt1+C[19]*pt2)*pv1 + (C[20]+C[21]*pt1+C[22]*pt2)*pv2 + (C[23]+C[24]*pt1+C[25]*pt2)*pv3$$

Where:

$$\begin{aligned}
 pv0 &= 1. \\
 pv1 &= vitnor \\
 pt0 &= 1. \\
 pt1 &= tetanor \\
 pv2 &= 2*vitnor*pv1 - pv0 \\
 pv3 &= 2*vitnor*pv2 - pv1 \\
 pt2 &= 2*tetanor*pt1 - pt0 \\
 pt3 &= 2*tetanor*pt2 - pt1
 \end{aligned}$$

Where:

$$\begin{aligned}
 tetanor &= (2.*x - (tetamin+tetamax))/(tetamax-tetamin) \\
 vitnor &= (2.*V - (vmax+vmin))/(vmax-vmin) \\
 tetamin &= 18. \\
 tetamax &= 58. \\
 vmin &= 3. \\
 vmax &= 25.
 \end{aligned}$$

Coefficients C are given by

$$\begin{aligned}
 C[0] &= 0.0 \\
 C[1] &= -2.437597 \\
 C[2] &= -1.5670307
 \end{aligned}$$

C[3] = 0.3708242
C[4] = -0.040590
C[5] = 0.404678
C[6] = 0.188397
C[7] = -0.027262
C[8] = 0.064650
C[9] = 0.054500
C[10] = 0.086350
C[11] = 0.055100
C[12] = -0.058450
C[13] = -0.096100
C[14] = 0.412754
C[15] = 0.121785
C[16] = -0.024333
C[17] = 0.072163
C[18] = -0.062954
C[19] = 0.015958
C[20] = -0.069514
C[21] = -0.062945
C[22] = 0.035538
C[23] = 0.023049
C[24] = 0.074654
C[25] = -0.014713